JGS
Journal of the Geological Society

Research article

Published Online First

doi:10.1144/jgs2016-018

Basin-scale architecture of deeply emplaced sill complexes: Jameson Land, East Greenland

Christian Haug Eide[1,2]*, Nick Schofield[3], Dougal A. Jerram[4,5,6] & John A. Howell[3]

[1] Department of Earth Science, University of Bergen, Box 7803, 5020 Bergen, Norway
[2] Centre for Integrated Petroleum Research, Uni Research CIPR, Box 7810, 5020 Bergen, Norway
[3] School of Geosciences, Meston Building, University of Aberdeen, Aberdeen AB24 3UE, UK
[4] Centre for Earth Evolution and Dynamics (CEED), Postbox 1028, Blindern, N-0315 Oslo, Norway
[5] DougalEARTH Ltd, Solihull B91 3NU, UK
[6] Earth, Environmental and Biological Sciences, Queensland University of Technology, Brisbane, QLD 4000, Australia
* Correspondence: christian.eide@uib.no

Abstract: Igneous sills are common components in rifted sedimentary basins globally. Much work has focused on intrusions emplaced at relatively shallow palaeodepths (0 – 1.5 km). However, owing to constraints of seismic reflection imaging and limited field exposures, intrusions emplaced at deeper palaeodepths (>1.5 km) within sedimentary basins are not as well understood in regard to their emplacement mechanisms and host-rock interactions. Results from a world-class, seismic-scale outcrop of intruded Jurassic sedimentary rocks in East Greenland are presented here. Igneous intrusions and their host rocks have been studied in the field and utilizing a 22 km long 'virtual outcrop' acquired using helicopter-mounted lidar. The results suggest that the geometries of the deeply emplaced sills (*c.* 3 km) are dominantly controlled by host-rock lithology, sedimentology and cementation state. Sills favour mudstones and even exploit centimetre-scale mudstone-draped dune-foresets in otherwise homogeneous sandstones. Sills in poorly cemented intervals show clear ductile structures, in contrast to sills in cemented units, which show only brittle emplacement structures. The studied host rock is remarkably undeformed despite intrusion. Volumetric expansion caused by the intrusions is almost exclusively accommodated by vertical jack-up of the overburden, on a 1:1 ratio, implying that intrusions may play a significant role in uplift of a basin if emplaced at deep basinal levels.

Supplementary materials: Uninterpreted versions of Figures 7, 8 and 11 are available at http://doi.org/10.6084/m9.figshare.c.3281882

Received 3 February 2016; **revised** 9 June 2016; **accepted** 10 June 2016

Igneous intrusions are common in many sedimentary basins worldwide, and are particularly developed in rifted passive and volcanic margins, where rifting can lead to melt production and/or where rifting is also associated with flood basalt emplacement and large igneous provinces (e.g. Jerram & Widdowson 2005; Jerram & Bryan 2015). Sills injected into sedimentary sequences can have a profound impact on basin history, hydrocarbon migration pathways and reservoir properties, both at the time of emplacement and as a legacy of their structure long after their emplacement has ended (e.g. Holford *et al.* 2013; Schofield *et al.* 2015). During the last few decades, the study of igneous intrusions mainly in 3D seismic data has led to the realization that sill networks play a major role in magma transport within the crust (e.g. Larsen & Marcussen 1992; Cartwright & Hansen 2006; Schofield *et al.* 2015; Magee *et al.* 2016).

Intrusions emplaced at relatively shallow palaeodepths (<1.5 km) commonly have saucer-shaped geometries and are relatively well understood as they have been the focus of many studies based on work from field (e.g. Schofield *et al.* 2010; Hansen *et al.* 2011), seismic reflection (e.g. Planke *et al.* 2005; Hansen & Cartwright 2006; Schofield *et al.* 2015), theoretical (Polteau *et al.* 2008) and experimental (Galland *et al.* 2009) datasets. However, the emplacement mechanisms and geometry of intrusions that were emplaced at deeper basinal levels (>1.5 km), which show generally more planar characteristics (Planke *et al.* 2005; Hutton 2009; Schofield *et al.* 2012*a*), are much less well understood than those of their shallower counterparts. There are a number of reasons for this. Within seismic reflection data, deeper intrusions are commonly poorly imaged as they are often masked by shallow intrusive or extrusive rocks (e.g. basalt lava flows). Only a few detailed outcrop studies of large sheet intrusions emplaced at deeper basin depths have been published (e.g. Hutton 2009), owing in part to the difficulty in accessing large-scale outcrops of such rocks worldwide. Because of this, much of what is published about large-scale geometries of deep intrusions in sedimentary basins is based on theoretical considerations (e.g. Baer 1995) and limited sill exposures from small outcrop examples (e.g. Schofield *et al.* 2012*a*, 2016).

This lack of data and information about deep-seated basinal intrusions is potentially problematic. New seismic data from the frontier hydrocarbon basins such as the NE Atlantic have shown that sedimentary basins may contain extensive series of planar intrusions towards the base of the basin fill (Schofield *et al.* 2015), which can potentially lead to issues with compartmentalization of reservoirs and disruption of hydrocarbon migration pathways between source rock intervals and reservoirs. The larger sheet-like intrusions in deeper parts of basins will also play a part in the geotectonic evolution of the basin and its maturation history. Additionally, where sills occur in basins uplifted and eroded subsequent to sill intrusion, sill morphologies will reflect the original emplacement depths and conditions (Schofield *et al.* 2012*a*). Therefore the correct interpretation of these morphologies, in absence of other depth data such as burial curves, can give crucial insight in determining emplacement depths at which the magma intruded.

To address these issues, we present the results from a study of combined helicopter-lidar and outcrop datasets from a 22 km long and *c.* 250 m thick section of heavily intruded Early Jurassic sedimentary rocks of the Neill Klinter Group in the Jameson Land Basin in East Greenland (e.g. Larsen & Marcussen 1992; Hald & Tegner 2000; Figs 1 and 2). This section was at an approximate depth of 3 km at the time of magma emplacement of the Jameson Land Suite, constrained by

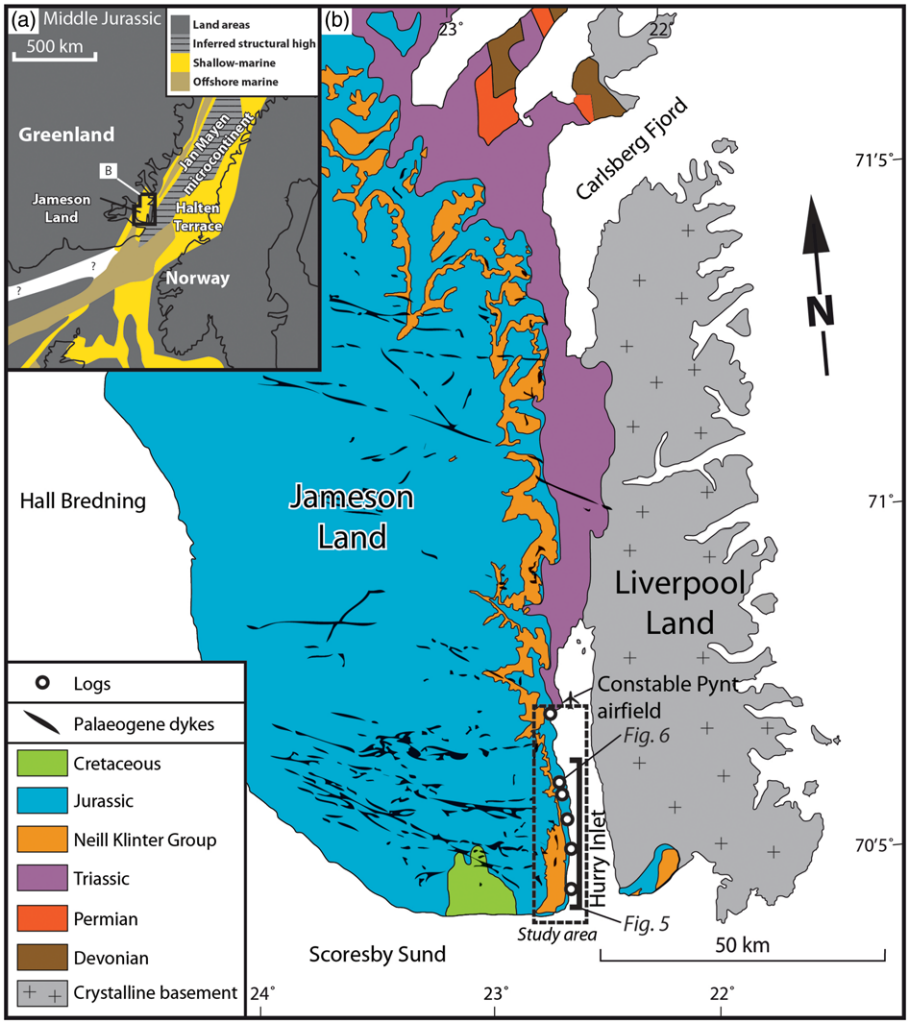

Fig. 1. Maps of the study area. (**a**) Pre-drift reconstruction of the seaway between Norway and Greenland at time of deposition of host-rock sediments (Middle Jurassic), modified from Ziegler (1988) and Doré (1992). (**b**) Geological map of the study area, modified from Ahokas *et al.* (2014*a*) with dyke intrusions from Noe-Nygaard (1976).

burial history curves based on a variety of data (e.g. Larsen & Marcussen 1992; Mathiesen *et al.* 2000; Hansen *et al.* 2001). The section is at a scale comparable with that for typical offshore seismic data, but includes data from extensive outcrop work including six logs, and at the decimetre scale in the virtual outcrop model (Eide *et al.* 2016). The combination of detailed logs and the high-resolution lidar model facilitates recognition of magma emplacement features that reveal the mode of emplacement, such as steps, bridges, fingers and peperites (Fig. 3).

The aims of this contribution are five-fold: (1) to document the large-scale architecture of intrusions in the Neill Klinter sea cliffs in Jameson Land; (2) to document structural features that reveal the mechanism of propagation of the sills; (3) to discuss the implications of these observed geometries in light of existing models of sill emplacement, propagation and overall magma transport; (4) to compare these observations with similar intruded systems world-wide; (5) to discuss the influence of deep igneous intrusions on petroleum systems within sedimentary basins, in terms of source and reservoir intervals, migration pathways, traps and imaging.

Background

Geological history of the Jameson Land Basin

During the Devonian a series of north–south-trending extensional basins formed between present-day Norway and Greenland as a result of post-Caledonian rifting (Surlyk 2003). The Jameson Land Basin is the southernmost of these, and is filled by up to 17 km of sedimentary rocks (Larsen & Marcussen 1992; Figs 1 and 2). The studied host-rock interval was deposited during a post-rift thermal-sag phase in the Early Jurassic, following a Triassic rift phase (Surlyk 2003, Fig. 4). Relative sea-level rise in the latest Pliensbachian led to marine flooding of the basin and deposition of the Neill Klinter Group in a mainly tide-influenced, shallow-marine, structurally controlled embayment (Dam & Surlyk 1998; Eide *et al.* 2016; Fig. 1a). The Neill Klinter Group is time-equivalent and analogous to the prolific reservoir rocks on the conjugate Halten Terrace offshore Norway (Martinius *et al.* 2001; Ichaso & Dalrymple 2014), and was deposited in a minor sub-basin in the narrow, tide-dominated seaway that occupied the rifted continental crust between present-day Norway and Greenland (Gjelberg *et al.* 1987; Fig. 1a).

The tide-dominated delta of the Elis Bjerg Member (Ahokas *et al.* 2014*a*; Eide *et al.* 2016) mainly consists of sandy heteroliths (Fig. 5), which are brittle, well-cemented, dominantly sandy deposits comprising interbedded sandstone and mudstone, with sandstone beds generally ranging from 1 to 60 cm thick, and mudstone beds and laminae ranging from 0.1 to 10 cm thick (Fig. 6). The outcrop is oriented obliquely along-strike of this delta system, and the southern part is further away from an inferred sediment input point located to the west of Harris Fjeld (Fig. 1), leading to gradually more distal and mudstone-rich deposits in the south part of the study area (Dam & Surlyk 1998; Eide *et al.* 2016; Fig. 5). Further sea-level rise led to gradual backstepping and later abandonment of the deltaic system in the study area, and deposition of the dark, mudstone-rich, offshore deposits of the Albuen Member (Dam & Surlyk 1998; Eide *et al.* 2016). A rapid forced progradation of the shallow-marine system

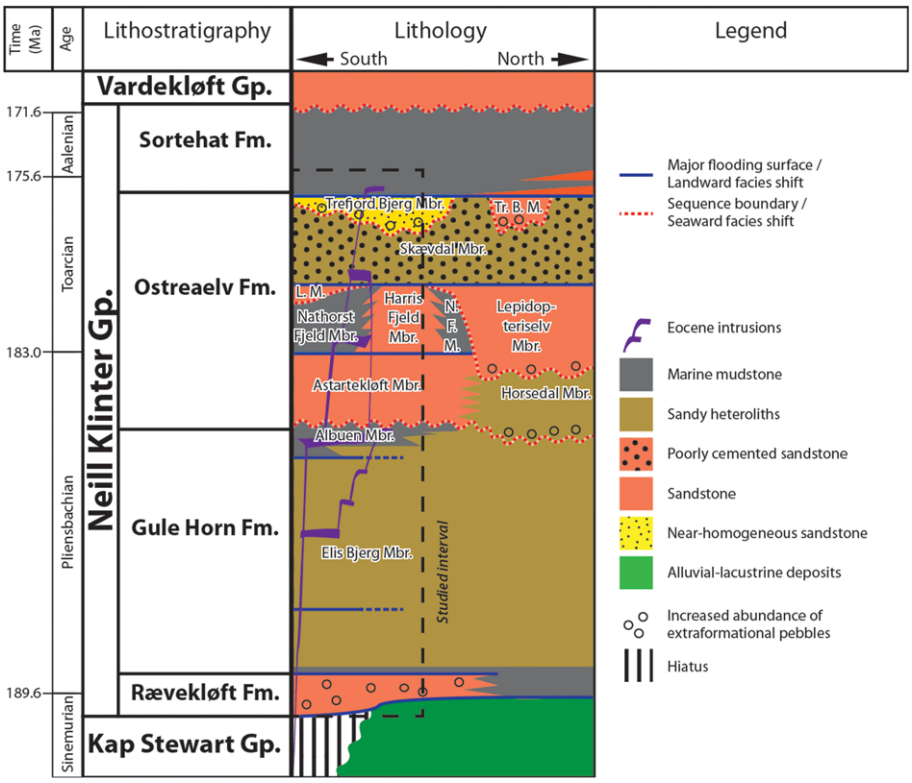

Fig. 2. Lithostratigraphy of the study area. Modified from Ahokas *et al.* (2014*a*) and Eide *et al.* (2016).

marks the erosive, lower boundary of the Astartekløft Member of the Ostreaelv Formation, which mainly consists of thick, sandstone-dominated, cross-bedded tidal dunes (Dam & Surlyk 1998; Ahokas *et al.* 2014*a*,*b*). The overlying Nathorst Fjeld Member mainly consists of clay-rich, light grey sandstone, interpreted to have been deposited in a stressed, brackish embayment (Ahokas *et al.* 2014*a*). This is further overlain by the well-cemented, pebbly sandstones of the Lepidopteriselv Member, interpreted as an incised valley deposit (Ahokas *et al.* 2014*b*). The following Skævdal Member consists of intensely bioturbated, poorly cemented heteroliths (Figs 5 and 6). The low degree of cementation of this unit is caused by extensive chlorite coating of the quartz sand grains (Ahokas *et al.* 2014*a*). This interval is further overlain by the thick, homogeneous, well-cemented, cross-bedded sandstones, with occasional mudstone drapes on foresets, of the Trefjord Bjerg Member, interpreted as the deposits of estuarine tidal dunes (Ahokas *et al.* 2014*a*). The uppermost part of the studied deposits consists of the dark, organic-rich, offshore mudstone of the Sortehat Formation (Krabbe *et al.* 1994; Stemmerik *et al.* 1998).

Volcanic history of East Greenland and the Jameson Land Basin

The opening of the North Atlantic gave rise to the extensive Paleocene and Eocene igneous rocks in West Greenland, NW Britain and at the conjugate East Greenland–NW European margins (e.g. Saunders *et al.* 1997; Hansen *et al.* 2009; Jerram *et al.* 2009; Brooks 2011; Nelson *et al* 2015). Along East Greenland this opening propagated northwards to the Norwegian–Greenland Sea and led to plate separation occurring during the Eocene (*c.* 55 Ma), and was accompanied by widespread igneous activity along 2000 km of the conjugate rifted margins (e.g. Brooks 1973, 2011). This led to the extrusion of a thick volcanic series, dominantly subaerial lava flows, of which more than 2 km are still exposed in the Geikie Plateau south of Jameson Land today (Larsen *et al.* 1989; Brooks 2011). This volcanic package thins towards the north, and reached a thickness of *c.* 1 km in the study area, but is now completely eroded there (Mathiesen *et al.* 2000). The sedimentary rocks of the Jameson Land Basin are cross-cut by WNW–ESE-trending dykes (Fig. 1b), which range from 1 to 10 m in width. The section is also intruded by broadly layer-parallel sills (Fig. 5; Larsen & Marcussen 1992; Hald & Tegner 2000). Throughout the North Atlantic Igneous Province it can be shown that there are two main periods of igneous activity, with ages of *c.* 62 – 58 Ma and *c.* 57 – 53 Ma, with detectable peaks at *c.* 60 Ma and at *c.* 55 Ma, respectively (Saunders *et al.* 1997; Torsvik *et al.* 2001; Jerram & Widdowson 2005; Hansen *et al.* 2009; Brooks 2011, and references therein). These are often cited as relating to the impingement of the Iceland plume and the main phase of rifting and continental separation (Hansen *et al.* 2009).

In Jameson Land, the volcanic episode is akin to the second pulse of activity in the North Atlantic Igneous Province. The majority of sills and dykes in the study area consist of aphyric to sparsely porphyric tholeiitic dolerite with olivine and plagioclase micro-phenocrysts, and appear to be coeval and to have crystallized in a closed magma system from a single magma batch from the resultant composition and lack of cross-cutting relationships (Hald & Tegner 2000). These intrusive rocks yield ages of 53 – 52 Ma, and hence postdate main flood volcanism in the area by 2 – 5 Ma and inception of sea-floor spreading by 1 – 2 Ma, and are interpreted to have been emplaced during a failed attempt to shift the rift zone westwards (Hald & Tegner 2000), similar to the later, successful shift, which led to the separation of the Jan Mayen Microcontinent (e.g. Talwani & Eldholm 1977; Mjelde *et al.* 2008). These are cross-cut by a small number of narrow dykes consisting of biotite-bearing alkali basalts (Hald & Tegner 2000), but only one cross-cutting dyke has been observed within the study area. These are similar to alkaline intrusive centres just north of Jameson Land emplaced at 30 – 36 Ma, but unpublished dates suggest that these are closer in age to the main phase of tholeiitic intrusions (Hald & Tegner 2000).

Several lines of evidence show that the studied intrusions were emplaced at maximum burial of the host rock. Thickness of stratigraphic intervals in the region, corroborated by basin modelling constrained by maturity and apatite fission-track data, indicates that the host rock in the study area was buried to a depth of over 2 km by Middle Jurassic to Late Cretaceous strata, and a further

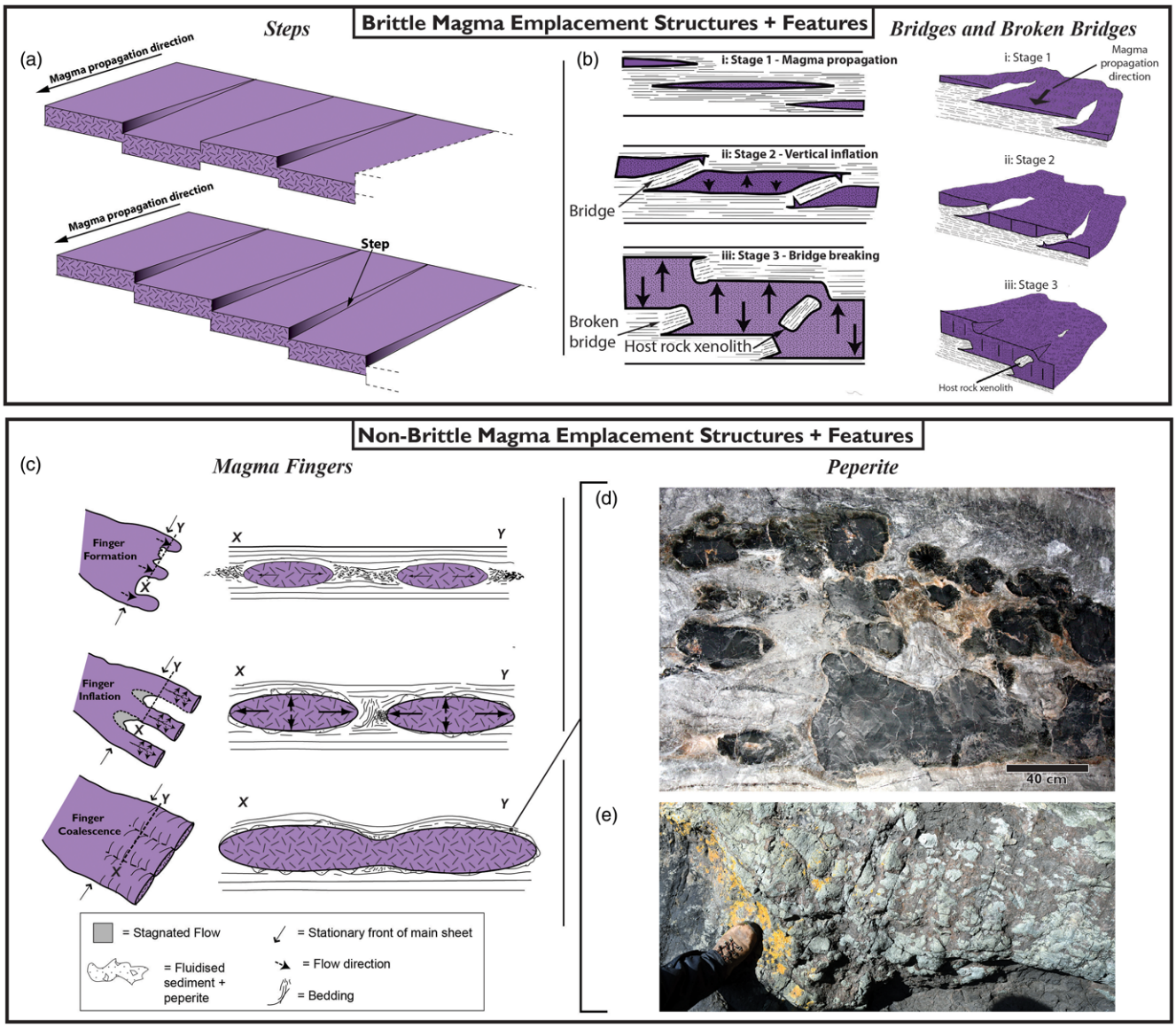

Fig. 3. Overview of sill structures and features formed during emplacement and progressive inflation of sill intrusions in brittle (**a**, **b**) and non-brittle (**c**–**e**) host rock. Modified from Schofield *et al.* (2012*a*). (**a**) Expression of steps on sill margins and how they relate to the magma propagation direction. (**b**) Development of broken bridges through vertical inflation of sills. (**c**) Development of magma fingers. (**d**) Example of peperite in salt from the Herfa–Neurode mine, Germany. (**e**) Peperite in shallow mudstone from Isle of Skye, UK.

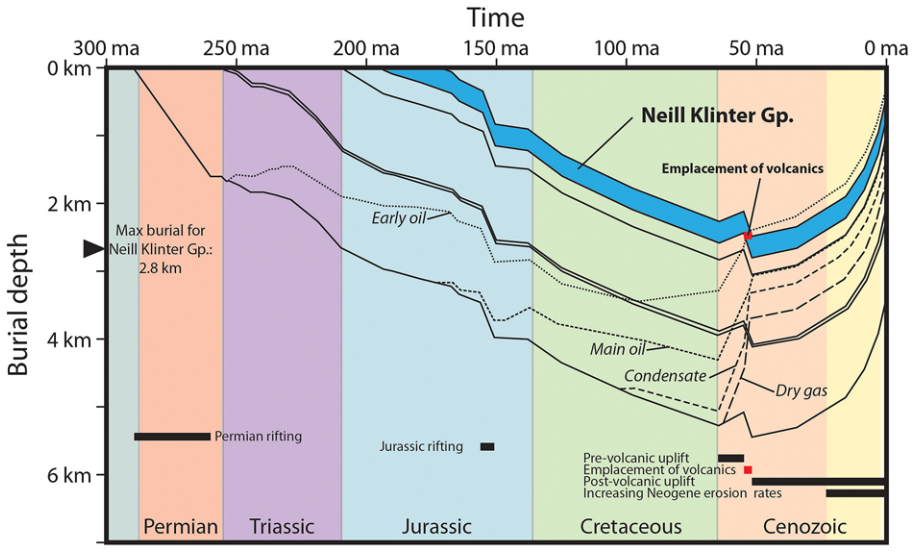

Fig 4. Simplified subsidence, uplift and hydrocarbon generation history for the studied parts of the Jameson Land Basin, constrained by maturity data and apatite fission-track analysis. Modified from Mathiesen *et al.* (2000).

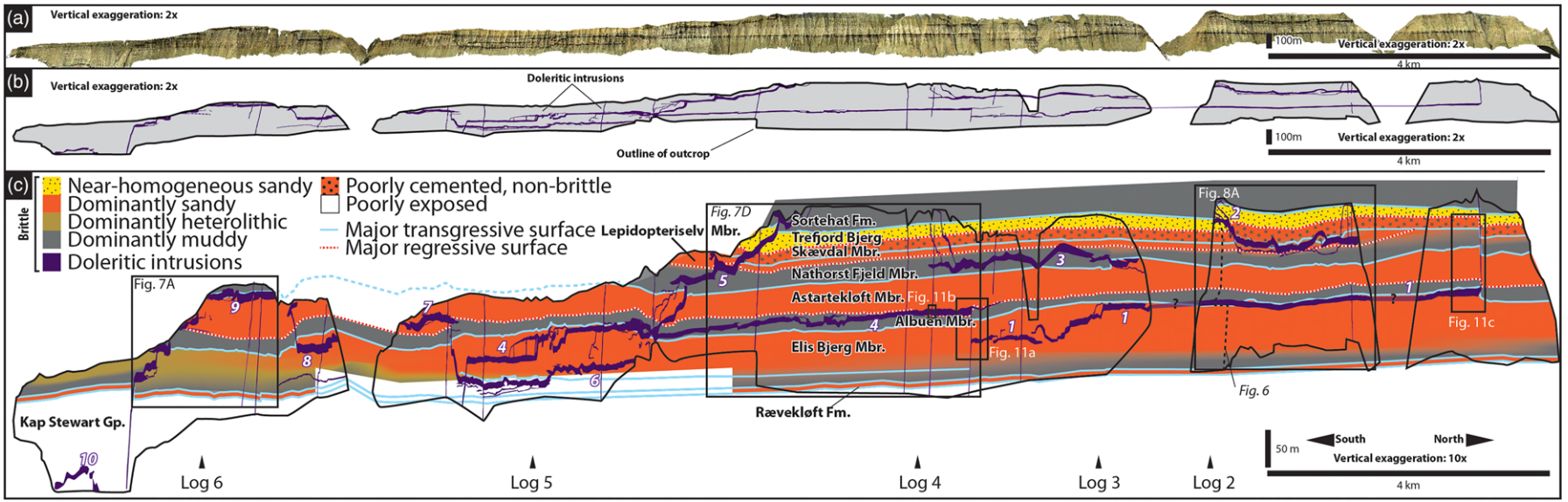

Fig. 5. Geometry of intrusions in the Neill Klinter Group along Hurry Inlet. (**a**) Virtual outcrop shown with 2× vertical exaggeration. (**b**) Outline of outcrops and geometry of intrusions with 2× vertical exaggeration. Sills are commonly *c.* 10 m thick, and major dykes are *c.* 4 m wide. (**c**) Vertically exaggerated (10×) panel showing geometry of sills, lithology and location of logs in the study area. The roughly layer-parallel geometry of the sills, striking jack-up of host rock above sills, and the tendency for intrusions to follow regional mudstones should be noted. Intrusions are labelled 1 – 10 from right to left for ease of reference.

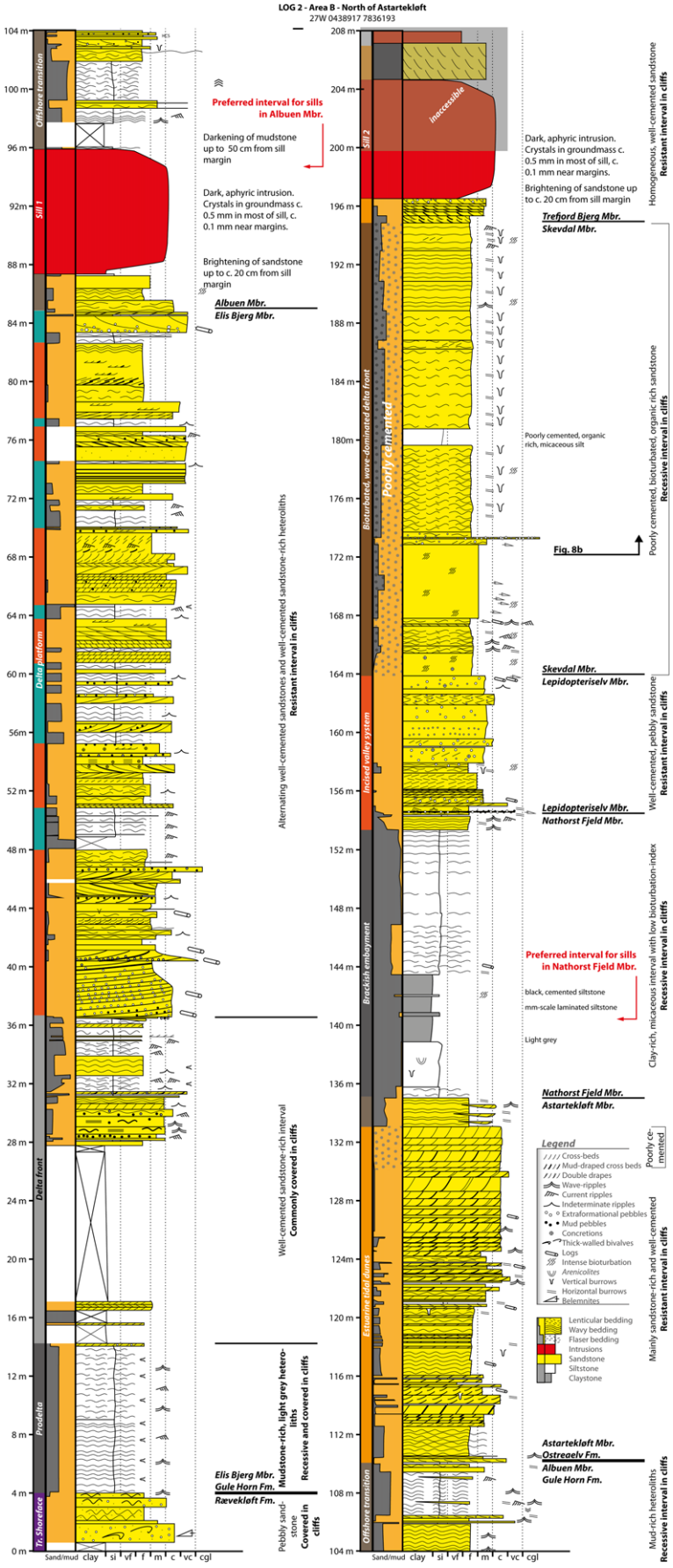

Fig. 6. Lithology of Neil Klinter Group in Log 2 (see Figs 5 and 9 for location). The pronounced differences between different lithostratigraphic units should be noted. The general patterns observed in this log are also valid for the rest of the study area, but host rocks are generally muddier towards the south. The mudstones of the Albuen (92 m) and Nathorst Fjeld (140 m) members are the most commonly intruded intervals.

c. 1 km of Paleocene to Eocene volcanic rocks before sill emplacement (Fig. 4; Mathiesen *et al.* 2000; Hansen *et al.* 2001). Thus, intrusion happened at *c.* 3 km below the contemporaneous land surface (Mathiesen *et al.* 2000). Since emplacement of igneous rocks, the basin has been subject to major uplift and erosion leading to removal of the entire Cretaceous section and exposure of the Jurassic interval within the study area (Mathiesen *et al.* 2000; Hansen *et al.* 2001).

Importantly, the maximum palaeotemperature of the Neill Klinter Formation prior to igneous emplacement is estimated to have been *c.* 100 – 120°C (Mathiesen *et al.* 2000; Fig. 4). Temperatures in this range are commonly associated with development of quartz cementation (see Oelkers *et al.* 1996), leading to a reduction in porosity and permeability, and increase in mechanical strength, suggesting that the studied sandstone units were already well cemented at the time of magma intrusion. The only exception to this is the Skævdal Member, which is characterized by a very low degree of cementation (Figs 5 and 6), as a result of an abundance of chlorite-coated sand grains that inhibited precipitation of quartz in these locations during burial (Ahokas *et al.* 2014*a*).

Sill emplacement mechanisms, morphology and relationship to host rock

Recent studies have shown that host-rock lithology and related properties have a critical influence on the emplacement and subsequent development of sills, resulting in an inherent link between emplacement mechanisms and resultant sill morphology (e.g. Schofield *et al.* 2012*a*; Fig. 3). Although several properties are important in this respect, a dominant factor is the mechanical strength of the host rock at the time of intrusion, and the host rock's ability to act in a brittle or non-brittle fashion during magma intrusion. In clastic rocks, this is controlled to a large degree by the state of consolidation and cementation within the host rock at the time of magma emplacement (Schofield *et al.* 2012*a*). The different mechanisms of magma emplacement, in the form of brittle or non-brittle emplacement, are manifested in different structures developed during intrusion, which can be used in outcrop to understand magma flow directions (Schofield *et al.* 2012*a*).

Emplacement structures that are commonly associated with brittle emplacement are steps and bridge structures. Steps form from initially offset en echelon fractures that later coalesce into a single sheet as fractures extend through magma inflation (Pollard 1973; Rickwood 1990). The offsets between the fractures are preserved as steps on sill margins (Fig. 3a). Each of the steps is therefore perpendicular to the direction of magma flow (Rickwood 1990; Schofield *et al.* 2012*a*). Seeing a series of clearly expressed steps that intersect the outcrop is indicative that magma flow was oriented in or out of the strike of the outcrop face. Bridges occur when separate intruding sills occur on slightly offset, but overlapping horizons. As the sills begin to inflate with magma, bending of the host rock between the two sills occurs, and the resulting structure is termed a bridge (Fig. 3b) (Hutton 2009). Under further inflation and bending, tensile cross-fractures may develop on the outer bends of these bridges, extending perpendicularly across the bridge (Fig. 3b). If inflation of the sills occurs to an extent that these magma-filled cross-fractures breach the bridge, the sills will become linked, and this structure is termed a broken bridge (Fig. 3b). Bridges and broken bridges seen clearly at outcrop cross-sections also indicate magma flow normal to the outcrop (Hutton 2009; Schofield *et al.* 2012*b*).

Host rocks with low mechanical strength and cohesion will often exhibit ductile or non-brittle behaviour during magma emplacement, which leads to development of a viscous–viscous interface between host rock and intruding magma, and formation of elliptical magma fingers, which can coalesce during later inflation (Fig. 3c) (Pollard 1973; Schofield *et al.* 2010). Intrusion into unconsolidated or poorly consolidated sediment can lead to a dynamic interaction between the magma and the sediments. This process forms a zone with incoherent, ragged or clast-like mixture of host sediment and igneous rock known as a 'peperite' (Fig. 3d and e; e.g. Skilling *et al.* 2002). Peperites and complex breccias commonly form where the unconsolidated sediment is wet (Skilling *et al.* 2002), but can also form in dry sediments (e.g. Jerram & Stollhofen 2002), and as a dynamic mixture of magma and host rocks in complex intrusions into evaporites, carbonates and coals (Schofield *et al.* 2012*a*, 2014). In this case additional fluids are generated by the reaction of the melt with the sediment, which can lead to enhanced fluid migration and brecciation along intrusion boundaries, and also lead to venting at sill tips to the surface (e.g. Jerram *et al.* 2016; Polozov *et al.* 2016).

Methods and dataset

The study area comprises the north–south-trending west side of Hurry Inlet in Jameson Land, from the exposures at Harris Fjeld to where the Neill Klinter Group is eroded near the confluence between Hurry Inlet and Scoresby Sund (Fig. 1). The dataset consists of six sedimentary logs with a total length of 1040 m and a photorealistic virtual outcrop model of the 22 km long outcrop belt acquired using oblique helicopter-mounted lidar scanning (Buckley *et al.* 2008; Rittersbacher *et al.* 2014; Eide *et al.* 2016), which captures the exposed part of the Neill Klinter Group below the Sortehat Formation (Fig. 2). The data were acquired using the Helimap System (Vallet & Skaloud 2004), using a laser scanner, a medium-format digital camera and a 35 mm lens, flying at a distance of *c.* 350 m from the cliffs. This yielded a model with point spacing of 0.3 m and image pixel resolution of *c.* 7 cm. The sedimentary logs collected at outcrop record grain size, sedimentary structures, nature of bed contacts, sand/mud ratio and degree of cementation. Log 2, which covers 198 m of the studied section, is presented here as this is the most complete and well-exposed section logged in the study area (Fig. 6). Lateral stratigraphic variability is relatively low, apart for a gradual southwards decrease in sandstone content, and this log gives a good impression of the lithologies present (see Ahokas *et al.* 2014*a*; Eide *et al.* 2016).

The outcrop is relatively straight along its strike, and only limited 3D control is provided by gullies and cross-cutting valleys. Palaeocurrents indicate sediment transport mainly towards the west, indicating that the outcrop belt is a strike-section through the depositional system (Eide *et al.* 2016). The outcrop section is nearly devoid of visible faults, and tectonic dip is on average 3°W.

Observations

The majority of the host rocks consist of brittle, well-cemented, layered, sandy heteroliths (interbedded thin sandstone and mudstone beds) and sandstone (Figs 5 and 6) predominantly in the Elis Bjerg and Astartekløft Members. A large proportion of the rock volume also comprises laterally extensive mudstone units, namely the Albuen Member, the Nathorst Fjeld Member and the lower, prodelta to delta-front part of the Elis Bjerg Member (Figs 5 and 6). The majority of the sills were emplaced within the brittle heteroliths and the mudstones (26 and 58%, respectively; Fig. 7). Subordinate amounts of sills also occur in the brittle, well-cemented and rather homogeneous sandstones of the Trefjord Bjerg Member (8%) and in the poorly cemented, intensely bioturbated sandstones of the Skævdal Member (9%, Figs 5, 6 and 8). The sills are 1 – 10 m thick, massive, dark, aphyric and nonvesicular, and consist of crystals with a diameter of *c.* 0.5 mm. Sill margins have generally finer grain sizes, with crystals smaller than *c.* 0.1 mm. Sill margins are sharp, and host rock in contact with the sills show white discoloration for *c.* 20 cm away from the sills for sandstones, and dark discoloration for *c.* 0.5 – 2 m away from the sills for mudstones.

Large-scale intrusive geometries and relationships

All igneous features in the sill-bearing part of the outcrop larger than *c.* 1 m are indicated in Figure 5. The intrusions have been arbitrarily labelled from 1 to 10 for ease of reference (Fig. 5c). The sills generally

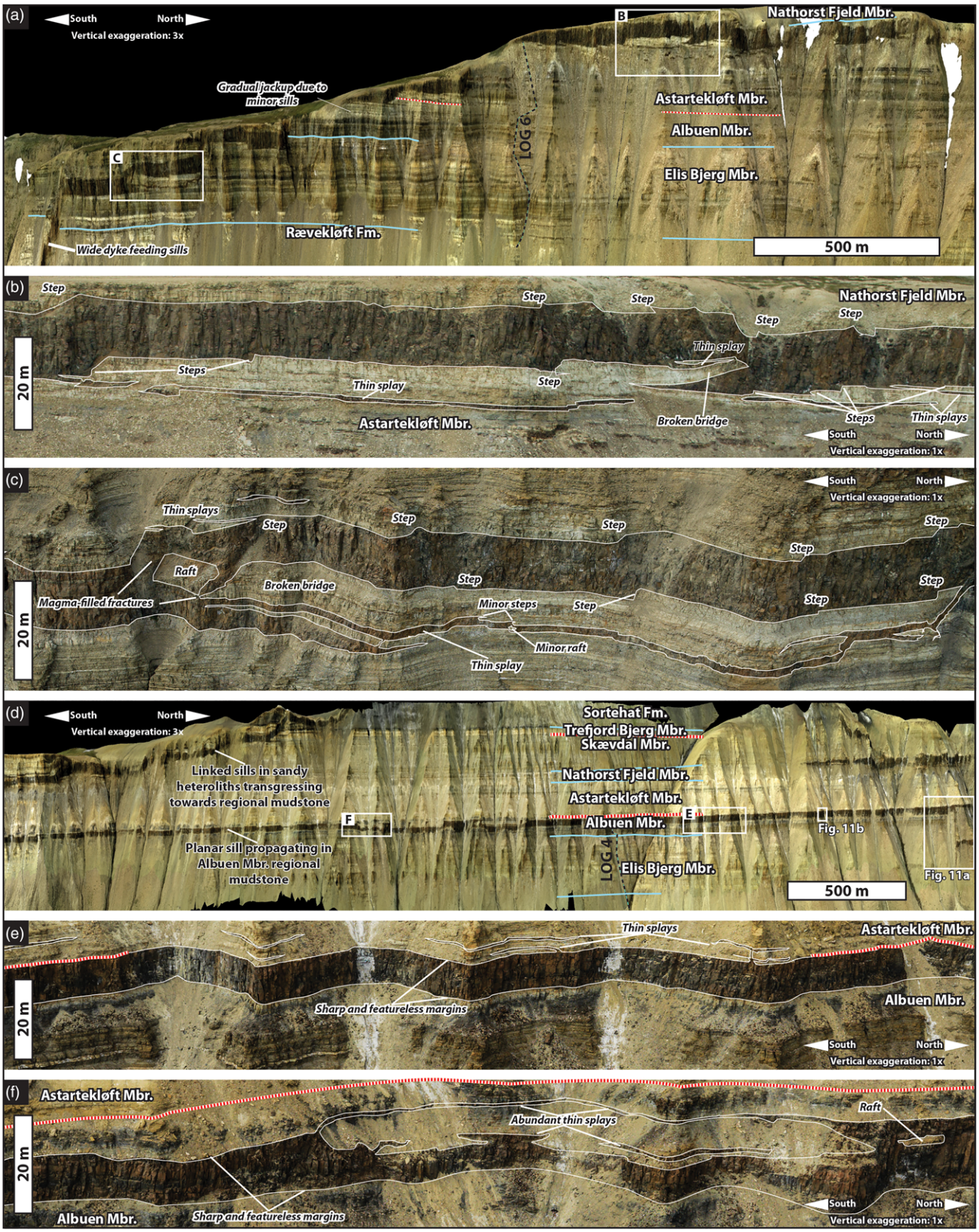

Fig. 7. Intrusion geometries and features in brittle heteroliths (**a**–**c**) and mudstone (**d**, **e**). (**a**) Overview of southernmost part of study area (see Fig. 5 for location). The wide dyke feeding a sill in the southern part, and the progressive upward stepping of the sill towards Nathorst Fjeld Member mudstone, should be noted. (**b**) Broken bridge and well-developed, smaller steps. These are the most common type of sill structures in layered, brittle host rocks in the study area. (**c**) Example of broken bridge and a raft. The abundant thin splays close to the main sill should be noted. (**d**) Overview of geometries of a tabular sill propagating in a regional mudstone (see Fig. 5 for location). The lateral persistence and vertical stability of the sill should be noted. (**e**) Typical expression of sill in the Albuen Member mudstone: sharp and featureless margins and small amounts of thin splays. (**f**) Uncommon expression of sill linkage in regional mudstone: sill shows featureless margins at main level, but exhibits significant amounts splays as it transgressed slightly downwards to a level *c.* 4 m below main level.

exhibit a layer-parallel geometry, which is expected for deeply intruded sills propagating in brittle host rock (Schofield *et al.* 2012*a*).

It is evident that the main sills are generally interconnected, because of a lack of cross-cutting relationships. Main sills are 7 – 12 m thick (9 m on average). Thinner splays (0.15 – 2.5 m thick) originate from the main sills, lie within 10 m of the main sills, and are parallel to these for several hundred metres. Main sills intersect each other and show complex splaying geometries near intersection points (Fig. 5).

The host rock is also intersected by 18 dykes (Figs 10a & 11) that are 1.1 – 9.6 m wide (median: 2.3 m). Only one is observed to cross-cut the sills (Fig. 11b); the rest are interpreted to be contemporaneous as they do not cross-cut the sills and are geochemically consistent (Hald & Tegner 2000). These are spaced 0.2 – 4 km apart, with an increasing spacing towards the north, and thus divide the host rock into intrusive-bounded blocks 0.2 – 4 km wide and 20 – 120 m thick. The sills make up *c.* 10% of the total present-day thickness of the studied outcrop, whereas the

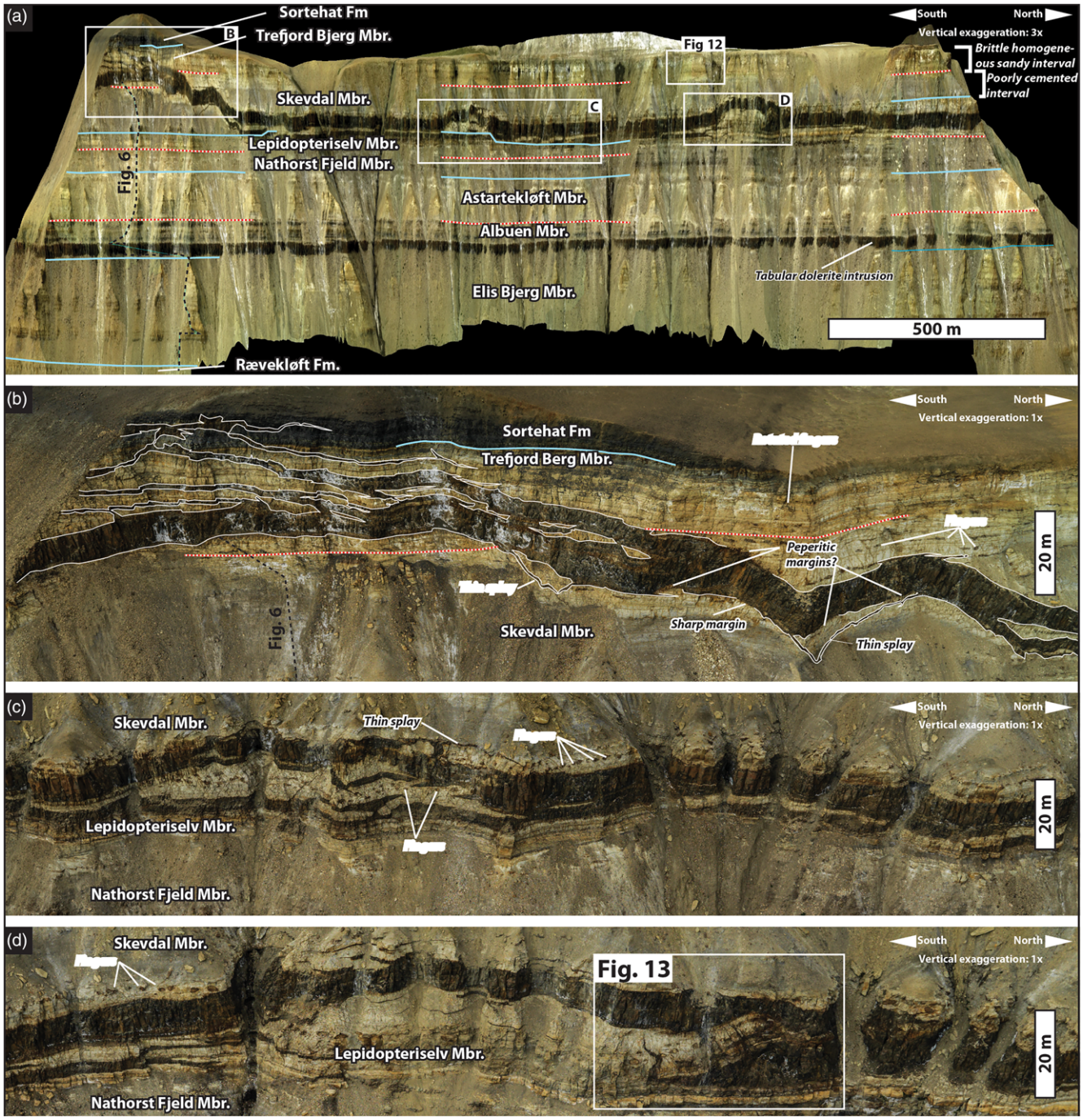

Fig. 8. Intrusion geometries and features in brittle homogeneous sandstone (**b**) and poorly cemented sandstone (**c**, **d**). (**a**) Overview of the area around Log 2 (see Fig. 5 for location). Noteworthy features are the tabular sill propagating in the Albuen Member mudstone, the regular buckling of the upper sill into the poorly cemented Skevdal Member (**c**, **d**), and the complex, divergent splays developed where the upper sill transgresses into the well-cemented, homogeneous sandstones of the Trefjord Bjerg Member (**b**). (**b**) Complex splaying geometries in the homogeneous, sandy Trefjord Bjerg Member, and simpler splays and peperitic margins in the underlying, poorly cemented sandstone of the Skevdal Member. (**c**) Sill propagating along the interface between the well-cemented Lepidopteriselv Member and the overlying, poorly cemented Skævdal Member. The abundant fingers and peperitic structures developed in the poorly cemented sandstones, indicating magma propagation in a partly non-brittle host rock, should be noted. (**d**) Another example of sill geometries in poorly cemented sandstone. The well-developed broken bridge, which is presented in further detail in Figure 13, should be noted.

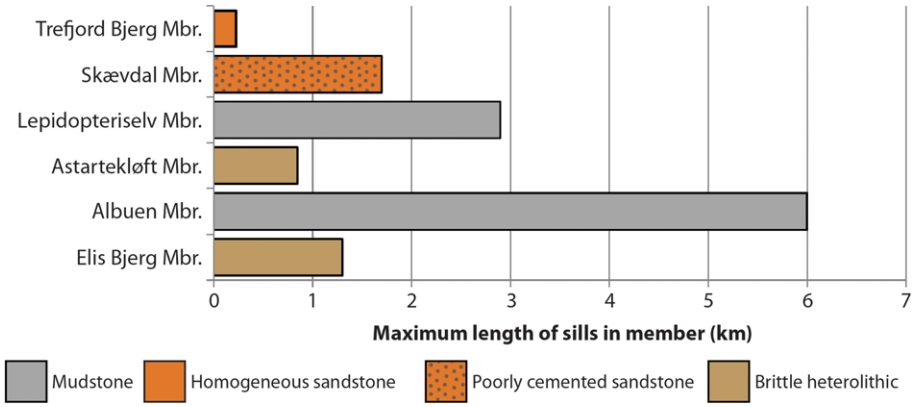

Fig. 9. Bar diagram showing maximum length of sills in the various members in the study area. The great length of sills in the regional mudstones, compared with the short maximum lengths attained in brittle homogeneous sandstone, and intermediate maximum lengths attained in brittle heteroliths and poorly cemented sandstone, should be noted.

dykes make up 0.2% of the total outcrop length in an north–south direction.

The sills are mainly layer-parallel and commonly follow stratigraphic discontinuities (Figs 5, 7d and 8a). The mudstone of the Albuen Member is the interval with the highest concentration of intrusions in the study area (Figs 5, 7d and 8a), and the sills occur most frequently in the basal part of this unit. The mudstone of the Nathorst Fjeld Member also contains a significant volume of sills (Fig. 5). Within the Nathorst Fjeld Member, the sills mainly occur in the central part of the mudstone unit, which is the most clay-rich interval in the study area (Fig. 6). Mudstone-dominated horizons within the Elis Bjerg Member associated with minor flooding surfaces (Eide *et al.* 2016) are also commonly exploited by sills (Fig. 5c). A small amount of intrusions are also present at the lower boundary of the poorly cemented Skævdal Member. The sills transgress (i.e. change stratigraphic interval) out of the sandier units over short distances, and are not emplaced to any significant degree within these units (Fig. 9).

Sills that intruded into the mudstone-rich Albuen Member remain concordant and strata-bound over lateral distances of up to 6 km, after which they terminate or transgress to another interval. This is in contrast to sills intruded into sandier units, which only remain strata-bound for relatively short lateral distances (<1.2 km) before transgressing subvertically (Figs 5 and 9). Within the heterolithic Elis Bjerg and Astartekløft members and the poorly cemented Skævdal Member, the sills stay strata-bound for *c.* 1 km. However, within the homogeneous sandstone of the Trefjord Bjerg Member, sills do not stay strata-bound for more than a few hundred metres. In the southern, more mudstone-rich part of the outcrop, a greater proportion of the sills is emplaced in the Elis Bjerg Member than in the northern half of the outcrop.

The host rocks show clear and well-defined jack-up above the sills in the investigated interval, as marker beds crossed by sills are offset by a thickness that equals the thickness of sills (Figs 5 and 10a). No faulting, folds or internal deformation structures are observed in the study area, indicating that the expansion of volume owing to sill emplacement was solely accommodated by jack-up of host rock, and not by localized host-rock deformation. This can be demonstrated, as it is possible to reconstruct the host-rock stratigraphy without any deformation simply by removing the sills in images taken orthogonally to the outcrop face and parallel to the plunge of the sills (Fig. 10b).

Sill morphology and structure

A detailed sedimentological description of the study interval has been given by Ahokas *et al.* (2014*a*) and Eide *et al.* (2016). For the purpose of the present study, four sedimentary lithologies are differentiated: well-cemented sandy heteroliths (Elis Bjerg and Astartekløft members), mudstone (Albuen and Nathorst Fjeld members), homogeneous sandstone (Trefjord Bjerg Member) and poorly cemented sandstone (Skævdal Member). Sill morphology and structure show significant variations across these four main lithologies, and these are considered separately below.

Sill emplacement and morphologies in layered sandy heteroliths (Elis Bjerg Member).

Sills that have propagated through the Elis Bjerg Member, which is dominated by brittle, sand-dominated, interlaminated sandstone and mudstone, commonly show steps along their length (Figs 7b and c; see Fig. 3b). Measured spacing between steps ranges from 20 to 80 m, and averages 30 m. The steps can be seen to exhibit *c.* 1 m of vertical offset.

Within the Elis Bjerg Member, separate sills are linked by broken bridges, which would have developed between separate intruding sills (see Fig. 3b). The prevalence of both steps and bridge structures in the sills shows that the current-day cliff face is oriented approximately perpendicular to the emplacement and magma flow axis of the sills (see Schofield *et al.* 2012*a*). The distance between separate broken bridges in sills emplaced within the Elis Bjerg Member is consistent at *c.* 200 m, suggesting that single magma lobes were uniform in width as they were propagating.

The broken bridges in the Elis Bjerg Member display cross-connecting magma-filled fractures that cut perpendicularly across the bridge structures (Fig. 7b and c). Completely isolated rafts of host rock, where cross-connecting fractures between two separate sills have isolated an entire raft of host rock, occur only in a minority of the exposed broken bridges (Fig. 8c), Unbroken bridges, which consist of deformed bridges of host rock separating two separate sills that are not broken by magma-filled fractures, but connected with host rock above and below the sills (Fig. 3b), are not observed in the study area.

Thin sill splays are commonly developed parallel to the main sills within the Elis Bjerg Member, and generally continue for a few hundred metres (Figs 5 and 7a, b). These commonly originate from discontinuities on the sill margins, such as steps or edges of sill-lobes at broken bridges. Splays commonly occur no further than 10 m above or below the sills. The majority of splays pinch out laterally over distances shorter than a few hundred metres (Fig. 7a–c). A few splays connect to other splays laterally, creating thin splays running parallel to and joining the main sill at both ends over *c.* 200 m (Fig. 7c). Some splays are observed to be isolated in the outcrop section, which indicates that the splays probably connect with other sill bodies outside the outcrop plane (Fig. 7b).

Sill emplacement and morphologies in regional mudstone intervals (Albuen and Nathorst Fjeld Members).

The highest proportion of sills observed in the study area, 58%, occurs within the regional mudstones of the Albuen and Nathorst

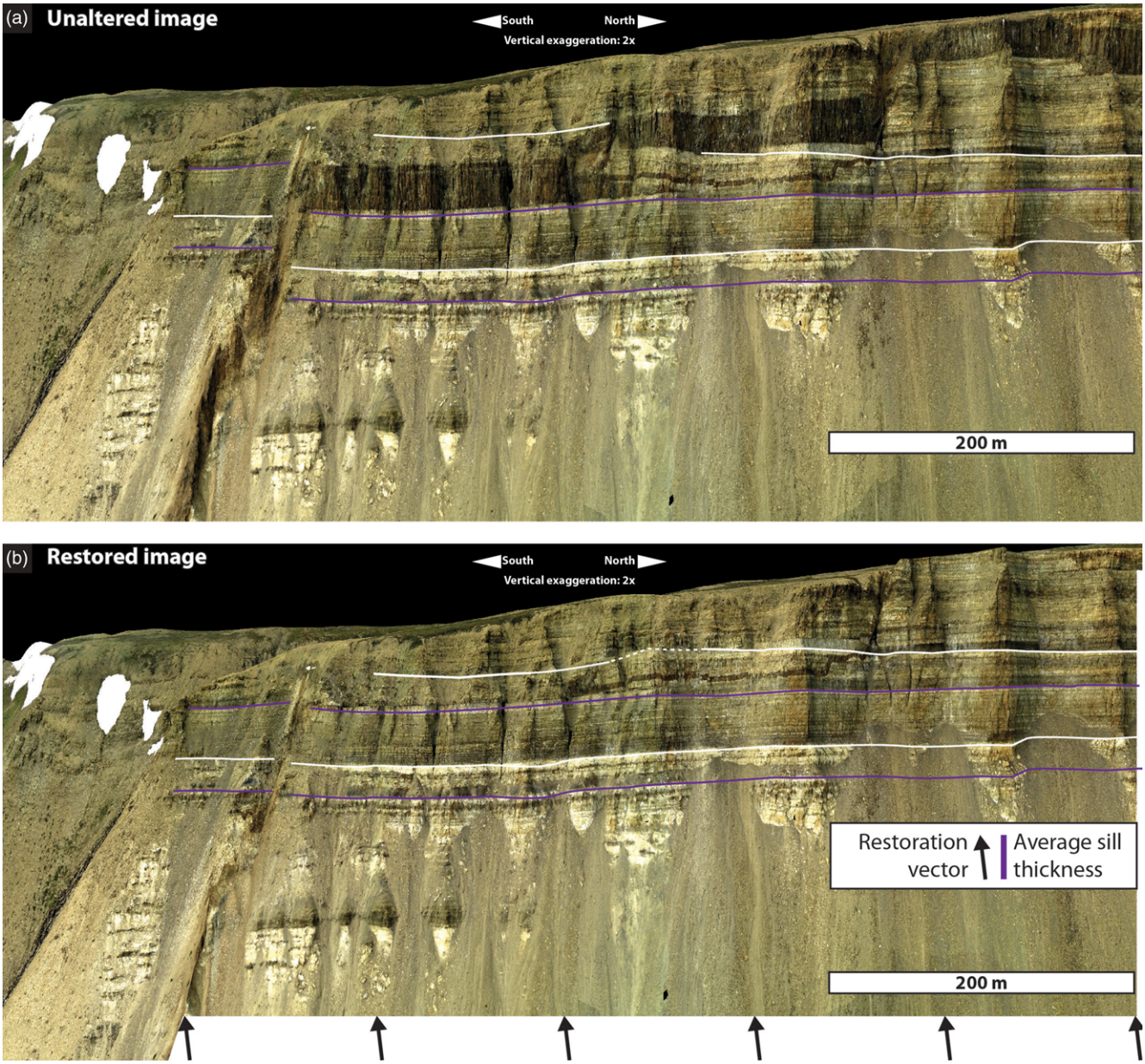

Fig. 10. Jack-up of host rock above intrusions. (**a**) Original image. The offset of the marker beds (black or white lines) equal to thickness of sill and lack of obvious host-rock deformation should be noted. (**b**) Reconstructed pre-intrusion geometry obtained by removing sill in image. The fact that the section restores without any visible deformation indicates that sill intrusion was accommodated solely by uplift of host rock equal to sill thickness, without significant host-rock deformation.

Fjeld members (Fig. 5). Sills that propagated in regional mudstones commonly exploited a preferred interval, generally the lowermost part of the Albuen Member, and the central part of the Nathorst Fjeld Member (Figs 5c and 7d). The preferred intervals correspond to the most fine-grained and clay-rich horizons in the regional mudstones (Fig. 6). Where the sill lies in a preferred interval, the sills are characterized by lateral strata-bound concordance over 1 – 6 km (Figs 7d and 8a). The contacts of the sills with host rock show mainly sharp and featureless margins, and have much more sparse and irregularly spaced broken bridge structures (0.1 – 1.7 km spacing, Fig. 8e and f) than sills propagating in the sandy heteroliths of the Elis Bjerg Member described above, suggesting that magma lobes or sills with a range of widths were propagating through the Albuen and Nathorst Fjeld members. Steps in sills propagating in muddy lithologies are limited to rare sub-metre examples with only minor amounts of thin sill splays developed around the margins.

In a few areas, the sills can be seen to locally have transgressed out of the preferred interval within the mudstone, into a horizon a few metres above or below (Fig. 7f). Where this relationship is observed, the main sill returned back into the preferred interval over a few hundred metres.

Sill emplacement and morphologies in brittle homogeneous sandstone (Trefjord Bjerg Member).

A low proportion (7%) of sills occur in the well-cemented, stacked cross-bedded sandstones of the Trefjord Bjerg Member (Dam & Surlyk 1998; Ahokas *et al.* 2014*a*). It is clear that the sills that have propagated in this member exhibit a very different morphology compared with the sills intruded into the other intervals. In one area (Fig. 8a), upon entering the Trefjord Bjerg Member, the sill has formed a complex interconnected network of sill splays 1 – 4 m thick (Fig. 8b). Well-defined broken bridges are not observed in this interval.

Interestingly, rotated magma finger structures are observed to occur in mudstone-draped cross-bed foresets and muddy toesets of

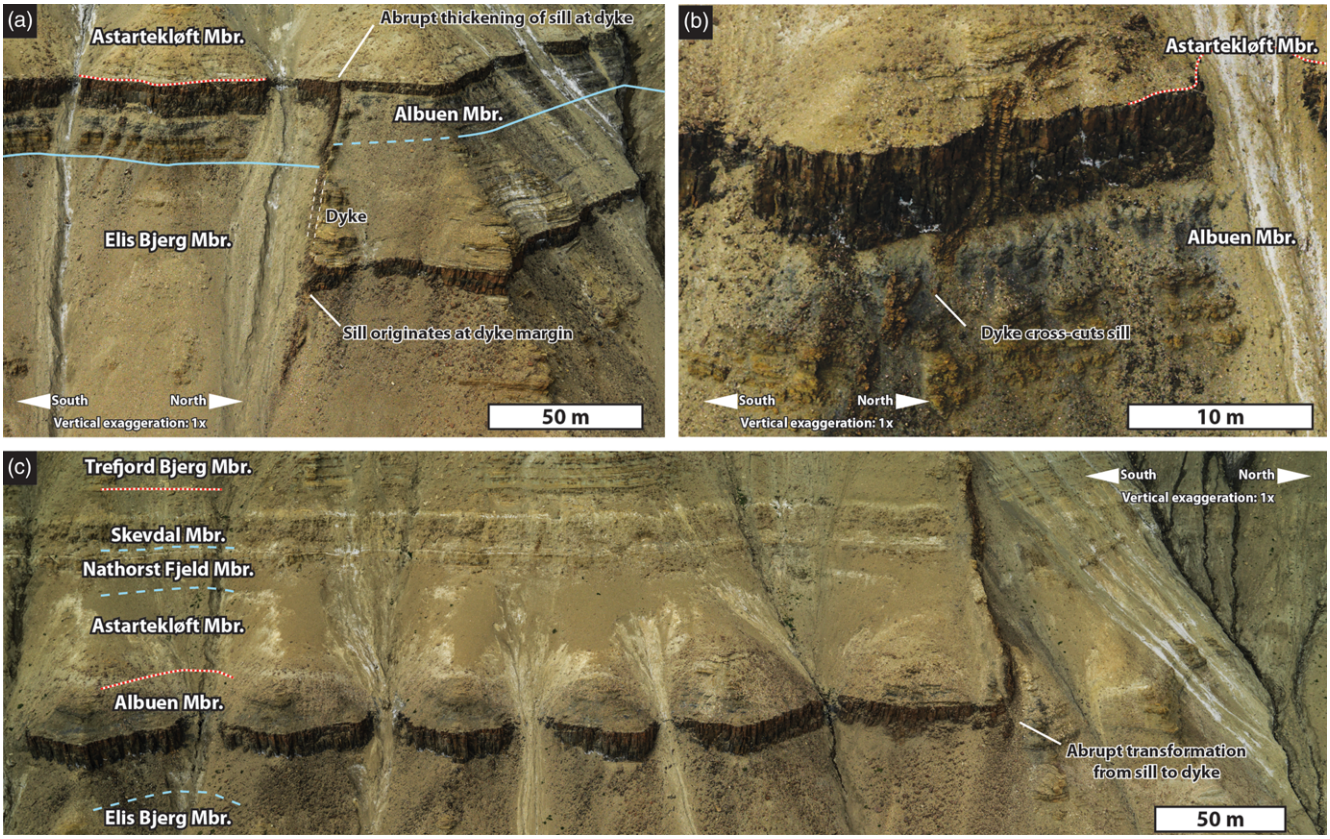

Fig. 11. Dykes in the study and their interaction with sills. The vast majority of dykes appear to be contemporaneous with the sills (**a**, **c**), but a small number of thinner (*c.* 2 m) dykes cross-cut sills (**b**). (See Fig. 5 for location.) (**a**) Near-vertical, 4 m thick dyke originates from below the outcrop and ends in the Albuen Member mudstone. The dyke feeds two sills, Sill 1 and Sill 4. (**b**) Sill is cross-cut by a later dyke. (**c**) Abrupt and apparently causeless transformation of Sill 1 from sill to dyke.

large tidal dunes (Fig. 12), indicating that the intrusions have tried to exploit any vestige of more mudstone-rich areas that occurs within this homogeneous sandy unit. The sills transgress out of this interval over distances shorter than 200 m, into the overlying organic-rich mudstone of the Sortehat Formation. This part of the outcrop has captured this process of sill migration dictated by sedimentary architecture in extreme detail, owing to the quality of the 3D data and the outcrop exposure.

Sill emplacement and morphologies in poorly cemented sandstone (Skævdal Member).

In the northern part of the study area, a *c.* 8 m thick and more than 1.8 km long sill is present at the interface between the well-cemented sandstones of the Lepidopteriselv Member and the poorly cemented, bioturbated sandstones of the Skævdal Member (Figs 5, 6 and 8a, c, d). Nine per cent of the sills occur within this lithology. The sill exhibits three occurrences of unusual upward buckling structures into the overlying poorly cemented sandstones at regular, 700 m, intervals along-strike (Fig. 8a). The southernmost of these 'buckles' resulted in transgression of the sill out of the Skævdal Member. The margins of the sill propagating at this interface have large amounts of thin splays close to the sill, and the parts of the sill that have intruded into the poorly cemented sandstone (commonly the upper surface) show elliptical magma fingers commonly 3 m wide and 1 m thick developed close to the sill (Figs 3c and 8c–d). Wispy, globular and incoherent intrusions on a centimetre to decimetre scale are interpreted as peperitic textures (*sensu* Skilling *et al.* 2002), and also occur in this interval (Fig. 13; see Fig. 3d and e). A broken bridge in this interval shows well-developed, magma-filled cross-fractures (Fig. 13), indicating brittle processes. However, in the same area the bridge structure also contains evidence of globular peperite, which indicates non-brittle processes of magma intrusion.

To our knowledge, such 'buckles' in sill geometry have not been described before. In this study, they are only observed in cross-section normal to the inferred magma flow direction, indicating that they are laterally propagating features aligned parallel to magma flow. They are propagating at regular intervals, and are probably associated with attempts to transgress out of the interval they are prograding in. Buckles occur only in the poorly cemented Skævdal Member, which indicates that they form exclusively in non-brittle rocks. As they have not been reported before in 3D seismic studies of relatively shallowly emplaced intrusions, it may be speculated that they represent structures that form in non-brittle rocks at high confining pressures.

Discussion

The role of sill splays in emplacement

Within the more hetrolithic units (e.g. Elis Bjerg Member) many of the sills are associated with numerous thin sills surrounding them; in some circumstances these appear to be 'splays' propagating away from the main sill bodies (e.g. Figs 7b, c and 8b). As the 'splay' morphology appears to be related to the more sand-rich units, compared with the more mud-rich horizons where the sills form planar bodies, this suggests that their formation is linked to the lithology.

Laterally intruding magma is known to preferentially exploit mudstone horizons (Mudge 1968) owing to the strong anisotropy of mudstone, which offers zones of weakness and parting horizons along the emplacement direction of the intruding magma

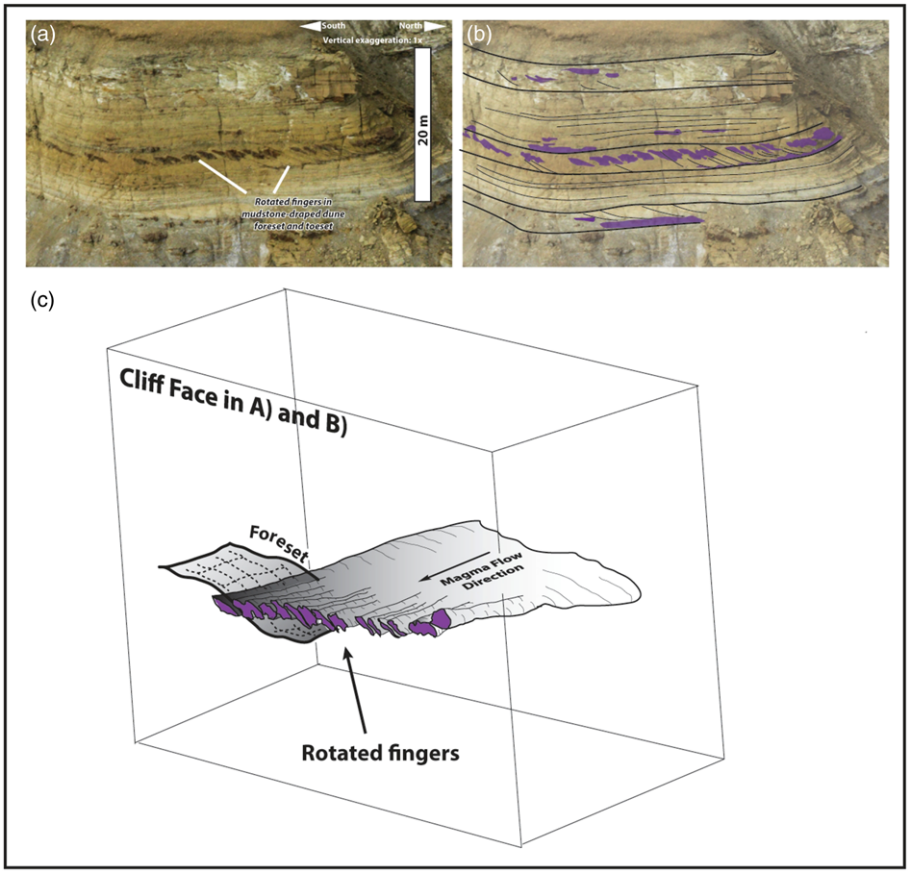

Fig. 12. Uninterpreted (**a**) and interpreted (**b**) view of thin intrusions into brittle, homogeneous sandstone in a tidal dune. The intrusions occur as thin 'rotated fingers' within mudstone-draped dune foresets and muddy dune toesets. This indicates that sills intruding into very homogeneous sandstone will exploit even very minor discontinuities. (**c**) A 3D illustration showing how the thin rotated fingers may relate to a thicker sill intrusion behind, or in front of, the outcrop face.

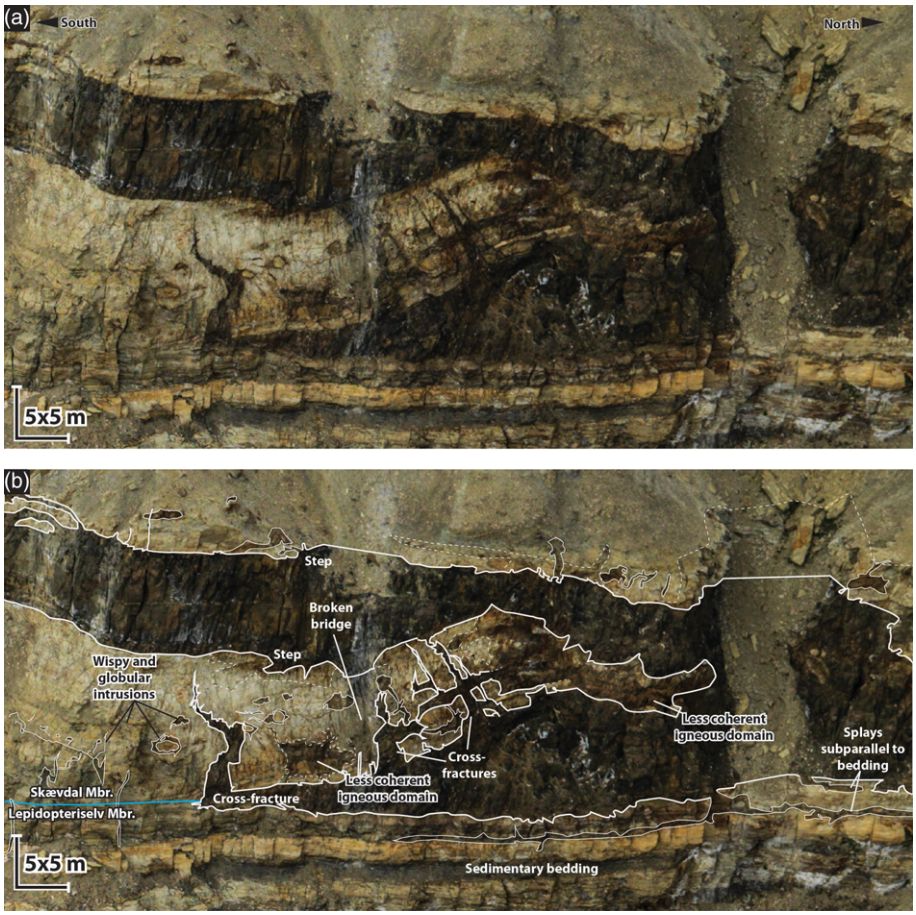

Fig. 13. Uninterpreted (**a**) and interpreted (**b**) close-up of a broken bridge with well-developed cross-fractures, developed at the interface between well-cemented heteroliths and poorly cemented sandstone (see Fig. 8d for location). The magma-filled fractures intruding vertically into the broken bridge, indicating that tensile fractures formed as the host rock was bent as the sills inflated, should be noted. Also noteworthy are the abundant non-coherent igneous domains, and wispy and globular features (peperite) developed in the poorly cemented Skævdal Member, and the layer-parallel and coherent intrusions into the layered rocks of the well-cemented Lepidopteriselv Member below.

(Kavanagh *et al.* 2006). However, within the more sand-rich units, such as the Trefjord Bjerg Member, substantial mudstone beds do not exist. It may be that the thin sill splays are initially formed as magma is propagating and splitting over several separate horizons, attempting to seek out a mechanically advantageous horizon to intrude along. At some point, one of the propagating sill splays may encounter a suitable horizon and thus becomes the dominant flow pathway and inflates (possibly owing to flow localization), essentially 'starving' the other smaller sills or splays of the majority of subsequent magma supply (Fig. 14). The final geometry therefore becomes one thick sill surrounded by several shorter, thinner sill splays.

Control of host-rock lithology on emplacement of sills

From the work presented here, host-rock lithology can be seen to play a critical role in sill morphology and emplacement sites. The sills within the study area can be seen to preferentially exploit and occupy the mudstones or discontinuities between strong and weak rocks. However, along-strike of the 22 km section, from south to north, the host rocks show lateral variations in sedimentary facies, which has resulted in differences of host-rock anisotropy. In particular, in the northern area of the section, the host rock is strongly anisotropic, with sharp division and contacts between mudstone and sandstone units. However, in the southern part of the section, the sandy units are more mud-rich, and there is therefore less of a lithological contrast between units. This aspect appears to have had an effect on the emplacement of the sills and large-scale sill morphology. In the northern strongly anisotropic section, the sills are almost exclusively seen in the 8 – 20 m thick regional mudstones, forming laterally planar coherent sills (over 3 – 6 km), with very little deviation or cross-cutting of stratigraphy (Fig. 5c). In the southern part of the section where the anisotropy between mudstone and sandy units is less well defined, a much larger volume of intrusions is present in the sandier units, with the intrusions displaying complicated morphologies, stepping up and cross-cutting stratigraphy. This is probably a result of a lack of strong lithological contrast to exploit or follow.

The state of consolidation of the host rock also appears to have played a controlling role in determining emplacement mechanism of the sills. All stratigraphic units, with exception of the Skævdal Member, are well consolidated, and were at their maximum burial depth (*c.* 3 km) at the time of magma emplacement (Fig. 4; Mathiesen *et al.* 2000; Hansen *et al.* 2001). This has resulted in magma intrusion in these sequences being dominated by brittle fracture processes, resulting in the formation of bridge and step structures, as the host rock was too cemented and mechanically strong to behave in a ductile manner. However, within the Skævdal Member, which is poorly consolidated and mechanically weak owing to the presence of chlorite overgrowths preventing cementation during burial, evidence exists for the formation of peperite. This is indicative of magma mingling with an unconsolidated host rock in a non-brittle fluidal manner (Skilling *et al.* 2002; Schofield *et al.* 2012*a*). Interestingly, the peperite is also found in close association with brittle structures, such as bridge structures with cross-connecting fractures (Fig. 13). This indicates that the rock was at the cusp of behaving in either a brittle or a non-brittle fashion and therefore, sensitive to the emplacement (and thus strain rate) of the intruding magma.

The field observations from Jameson Land illustrate that where (stratigraphic interval or horizon) and how (brittle or non-brittle) a sill intrudes appears to be governed to a large degree by the lithology of the host rock (see Schofield *et al.* 2012*a*), specifically its sedimentology. In particular, the relative amount and contrast of mudstone and sand beds, and also the level of consolidation or cementation of the beds at the time of intrusion appears to be a defining control. It is therefore crucial to understand the burial history, sedimentology and state of the host rock at time of intrusion in order to understand and predict the emplacement history and morphology of intrusions in areas of few data.

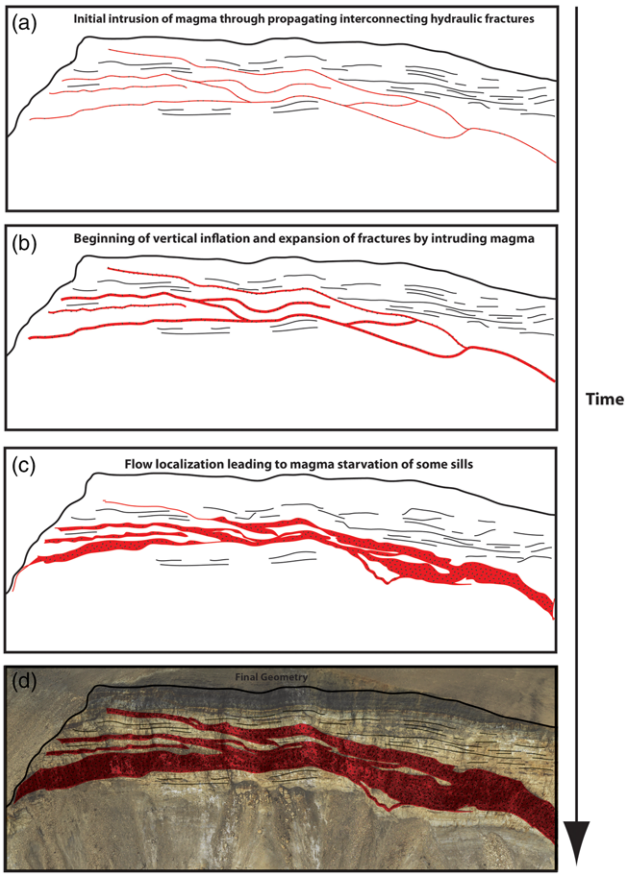

Fig. 14. Evolution of sills and splays through gradual inflation of interconnected fractures. (**a**) Initial intrusion of magma through propagating interconnected hydraulic fractures. (**b**) Beginning of vertical inflation of fractures by intruding magma. (**c**) Further inflation of sills. Flow localization leads to magma starvation in some sills, and greater inflation of more well-connected sills. (**d**) Further inflation of sills and final geometry.

Differential vertical intrusion-induced uplift in sedimentary basins

Previous studies of sill emplacement have found that in many cases, particularly in shallow intrusions (0 – 1.5 km), the vertical thickness of intruded magma is often accommodated partly by localized and internal host-rock deformation and that there is not a linear relationship between sill thickness and uplift or jack-up of overlying units (i.e. a 20 m thick intrusion does not result in 20 m of vertical uplift of overlying deposits) (Jackson *et al.* 2013; Schofield *et al.* 2014; Magee *et al.* 2016). In contrast, when any part of the studied section presented in this paper is reconstructed to its pre-intrusion geometry by removing sills from images, the sections restore with little change, with stratigraphy returning to pre-intrusion geometry (Fig. 10). Similar features are seen in other areas with sills intruded at great depths, such as those in Antarctica (e.g. Hutton 2009; Jerram *et al.* 2010), where there is little evidence of ductile deformation. This suggests that over the 22 km section in this study, the vertical thickness of the intruded sills has been accommodated largely by jack-up of the overlying strata in a near-linear 1:1 fashion (i.e. a 20 m thickness of intrusions lead to *c.* 20 m of jack-up). The likely reason for this linear relationship is, as discussed above, that the host

rocks that the sills intruded into were cemented and well lithified by the time of magma intrusion, and therefore did not have the ability to undergo localized deformation in the form of grain boundary deformation or pore-space collapse to accommodate the stress associated with the intrusion.

The behaviour seen within these deeper sills raises the interesting possibility that within a sedimentary basin that has undergone extensive sill intrusion, from shallow to deep basin levels, differential uplift could be associated with the intrusions vertically through the basin. Linear 1:1 uplift (jack-up) occurs at deep basinal levels (*c.* 1.5 km or deeper), changing into non-linear uplift above shallow-level intrusions (0 – 1.5 km), where much of the magma volume can be accommodated by localized internal host-rock deformation. In volcanic rifted margins, such as the Faroe–Shetland Basin, where there is a suggestion that the base of the basin fill is heavily intruded by a considerable thickness of laterally continuous tabular intrusions (Schofield *et al.* 2015), the potential exists for substantial uplift of the basin fill to occur regionally, which may not be easily attributable to intrusions because of the rapid decrease in quality and resolution of seismic reflection data with depth.

Comparison with other, well-studied examples of mafic sill intrusions

The studied intrusions of the Jameson Land Suite are emplaced in mainly brittle, well-cemented rocks at *c.* 3 km depth (e.g. Mathiesen *et al.* 2000), and the bulk of intrusions appears to have formed during a single episode of intrusion of tholeiitic magma that did not assimilate significant amounts of host rock (Hald & Tegner 2000). Furthermore, no coal or evaporite beds, which commonly attract sills as they are particularly mechanically weak (see Schofield *et al.* 2012*a*), are present. Other well-studied examples of mafic sill complexes are present in the Karoo Basin of South Africa, the Theron Mountains in Antarctica, and the San Rafael Swell area of eastern Utah, USA.

The majority of the exposed mafic intrusions in the Karoo Basin are generally saucer-shaped and emplaced at shallow levels; for example, *c.* 1.2 km below the contemporaneous surface (e.g. Polteau *et al.* 2008; Schofield *et al.* 2010). Here they have mainly intruded into very homogeneous, unstructured and relatively poorly cemented host rocks, which often display non-brittle sill structures (see Fig. 3), and are unlike the intrusions described in the present paper. Deeper sills, emplaced in the mud-dominated Ecca Group, are more tabular but these have received relatively little attention, owing to lack of exposure (Svensen *et al.* 2015). Examples do exist of saucer-shaped intrusions within more brittle host rocks such as lava sequences (e.g. Hansen *et al.* 2011). Here the emplacement is again shallow (within the flood basalt sequences), and the sills are initially sourced and propagated through thin sediment interbeds, highlighting a lithological control factor (Hansen *et al.* 2011).

The sills described from the Theron and Transantarctic Mountains in Antarctica show many similarities to the intrusions described in this paper (Hutton 2009; Jerram *et al.* 2010). They show abundant brittle emplacement structures such as broken bridges, bridges and steps, and are very laterally continuous sheet-like bodies. The sills complexes are also emplaced at a depth range of 2 – 4 km (Hersum *et al.* 2007; Jerram *et al.* 2010). However, they can attain thicknesses up to 330 m, and host-rock blocks show abundant melt trails, which indicate melting of the host rock (e.g. Hersum *et al.* 2007). The volume of intrusions is also much higher than in the studied section. This indicates that the sills in the Antarctica examples were associated with much larger volumes of magma emplacement.

Sills described from the San Rafael Swell area of eastern Utah are also laterally continuous, but are emplaced in a vertically homogeneous host rock, dominated by sand-rich units (Delaney & Gartner 1997). Sills here generally show lateral concordance over a kilometre scale (Delaney & Gartner 1997), and sill splays are common but show a much more chaotic and tangled morphology, probably as a result of sandstone-dominated host rocks and relatively poorly developed stratification. This highlights the critical role of host-rock properties on sill splay development.

In each of the above cases, the emplacement mechanisms and final morphology of the sills can be attributed to the state of the host rock at the time of intrusion. Although the saucer-shaped morphology seen in sills emplaced at shallow depths has received much investigation over the last 15 years (e.g. Planke *et al.* 2005; Hansen & Cartwright 2006; Polteau *et al.* 2008; Galland *et al.* 2009; Hansen *et al.* 2011), the mechanism by which the saucer-shaped morphology is formed appears to be quickly overridden by host-rock controls in the case of lithified host rocks.

Implications for hydrocarbon systems in intruded basins

Offshore NE Greenland has been the site of continuing hydrocarbon exploration interest, although understanding of this area is still sparse owing to the general limited coverage of seismic data and no current wells. The exact nature and extent of the Neill Klinter Group offshore has yet to be firmly established; however, it is clear that igneous intrusions occur through the Mesozoic in the offshore basins (e.g. Danmarkshavn Basin, Hamann *et al.* 2005). Within the studied section, the sills form a remarkably laterally continuous series of tabular intrusions, with the highest proportion of intrusion within the regional mudstone units of the Albuen and Nathorst Fjeld members. Sills in other, more brittle, intervals are still preferentially seeking out mudstones. Therefore offshore NE Greenland in, for example, the Danmarkshavn Basin, and in similar intruded basins worldwide, it could be expected that regional mudstone units are likely to be exploited by intrusions over tens of kilometres, including potential seals and middle to late Jurassic marine mudstones, which may form source rock intervals.

Observations from the field area show that where the more sand-rich units are cut by intrusions, they are associated with numerous smaller intrusions or splays cutting through the sequences (Fig. 8b), rather than just a single intrusion. This raises the possibility that in sedimentary basins where intrusions occur close to or cross-cut sand-rich reservoir sections, the reservoirs may actually be cut and segmented by numerous small intrusions rather than one large intrusion, potentially increasing the chance of creating barrier and baffles to fluid flow and hydrocarbon migration. Such behaviour will be difficult to see within the subsurface on seismic reflection data owing to limits in seismic resolution. When such features are imaged in seismic data, it may appear that a sill has terminated at a potential reservoir interval, whereas it may in fact simply have split into a series of thinner sill splays that are below the seismic resolution.

In most studies of offshore, subsurface intrusive complexes that utilize seismic reflection data, it is not possible to constrain the role of un-imaged vertical, dyke-like sources in transporting magma through the sedimentary fill of a basin (Schofield *et al.* 2015; Lecomte *et al.* 2016). This leads to the question of what potential role dykes may play in creating vertical fluid barriers in a sedimentary basin in areas where substantial sill intrusions can be seen.

From the 22 km section presented in this paper, 90 – 95% of the intrusive material visible in the section is in the form of sills, with only 5 – 10% represented by dykes. This suggests that within a sedimentary basin at depth, a strong bias will exist towards horizontal or bedding-parallel fluid barriers, rather than vertical fluid barriers. The exceptions to this would be within dyke swarms, which are more commonly associated with igneous centres (Jerram & Bryan 2015).

What would we see in subsurface seismic reflection data?

Although the intrusions in the 22 km section, which make up 10% of the total stratigraphic thickness, are laterally extensive and compartmentalize entire areas of the sedimentary section, the thickness of the single sills is relatively small (median 9 m, maximum 17 m).

In seismic reflection datasets, apart from at very shallow depths, vertical seismic resolution is typically in the region of 15 – 60 m (e.g. Cartwright & Huuse 2005; Magee *et al.* 2015). Thus, the small thickness of many of the sills within the section presented in this paper would in many subsurface scenarios be too thin to be resolvable, and they would be detected only as tuned reflection packages or not be detected at all (e.g. Schofield *et al.* 2015). This would certainly be the case in many offshore basins along the NE Atlantic Margin, where sill complexes are present at relatively deep levels in the contemporaneous basin fill (>3 km). However, seismic imaging of sills is strongly dependent on the dominant frequency of the seismic signal, overburden effects and processing parameters (e.g. Lecomte *et al.* 2016), and therefore what can and cannot be seen in seismic datasets is both dataset and basin specific.

Conclusions

This study has presented an exceptional quality 3D lidar dataset spanning a 22 km long and *c.* 250 m thick section. The detailed resolution of these data, and the exposures, has allowed the geometries and emplacement relationships of sill intrusions down to submetre scale to be investigated, with the following main findings.

(1) Lithological properties have a critical control on the style of emplacement of intrusions, shown by the concentrations of sills within certain levels of the stratigraphy and by the detailed lithological relationships within single sedimentary packages.
(2) Regional mudstone units are preferentially exploited by sills for several kilometres, and sills in such units show mainly sharp and featureless margins, and great vertical stability.
(3) In brittle, interlaminated sandstone and mudstone deposits, sills show well-defined and regular bridges and steps, and generally transgress towards regional mudstone units over *c.* 1 km.
(4) In brittle, homogeneous sandstones, sills transgress away from these intervals over a few hundred metres, and commonly splay into several sills 1 – 4 m thick.
(5) In poorly cemented sandstone deposits the sills show globular, chaotic and peperitic textures together with brittle structures such as bridges.
(6) Sills interconnect with dykes and have the potential to compartmentalize deposits into 'box-work' blocks of *c.* 2 km × 50 m.
(7) Despite the fact that sills significantly compartmentalize reservoir rocks and make up *c.* 10% of the thickness, the sills are generally too thin (*c.* 9 m) to be imaged by seismic survey at reservoir depths (kilometres).
(8) In contrast to sills emplaced at shallow levels, deeply emplaced intrusions (>1.5 km) show predominantly planar sill geometries and limited host-rock deformation.
(9) Stratigraphic reconstruction by removal of sills indicates that volumetric expansion owing to intrusion at deep levels in cemented rocks is accommodated almost exclusively by host-rock uplift.

In summary, this implies that significant igneous uplift can be attributed to large amounts of poorly imaged, deep sill intrusions, and highlights the importance of understanding the nature of igneous intrusions in volcanic rifted margins. This study shows that to predict sill geometries in the subsurface, it is crucial to understand the stratigraphy and sedimentology of the host rocks, the basin history and the timing of cementation relative to emplacement of intrusions. This is critical to better understand the evolution of basins along volcanic rifted margins and provide important constraints to allow successful hydrocarbon exploration and production in such settings.

Acknowledgements and Funding

We would like to thank reviewers S. Burchadt and S. Passey for the considerate and careful reviews, which improved this paper. Funding for data collection in this study was provided from the research council of Norway through the PETROMAKS project 193059 and the Force Safari project. Funding for data analysis was provided from PETROMAKS through the Trias North project (234152). D.A.J. is partly supported by research council of Norway Centres of Excellence funding (223272, CEED). The data were acquired by J. Vallet and S. Pitiot of Helimap Systems. S. Buckley is acknowledged for help with data processing, and G. Henstra and B. Nyberg for assistance in the field. A. Lynge and A. Andresen are thanked for logistical support.

Scientific editing by Andrew Carter

References

Ahokas, J.M., Nystuen, J.P. & Martinius, A.W. 2014*a*. Depositional dynamics and sequence development of the paralic Early Jurassic Neill Klinter Group, Jameson Land Basin, East Greenland: Comparison with the Halten Terrace, mid-Norwegian continental shelf. *In*: Martinius, A.W., Ravnås, R., Howell, J.A., Steel, R.J. & Wonham, J.P. (eds) *From Depositional Systems to Sedimentary Successions on the Norwegian Continental Shelf*. International Association of Sedimentologists, Special Publication, **46**, 291–333.

Ahokas, J.M., Nystuen, J.P. & Martinius, A.W. 2014*b*. Stratigraphic signatures of punctuated rise in relative sea-level in an estuary-dominated heterolithic succession: Incised valley fills of the Toarcian Ostreaelv Formation, Neill Klinter Group (Jameson Land, East Greenland). *Marine and Petroleum Geology*, **50**, 103–129.

Baer, G. 1995. Fracture propagation and magma flow in segmented dykes: field evidence and fabric analysis, Makhtesh Ramon, Israel. *In*: Baer, G. & Heinmann, A.A. (eds) *Physics and Chemistry of Dykes*. Balkema, Rotterdam, 125–140.

Brooks, C.K. 1973. Rifting and doming in southern East Greenland. *Nature Physical Sciences*, **244**, 23–24.

Brooks, C.K. 2011. *The East Greenland rifted volcanic margin*. Geological Survey of Denmark and Greenland Bulletin, **24**.

Buckley, S.J., Vallet, J., Braathen, A. & Wheeler, W. 2008. Oblique helicopter-based laser scanning for digital terrain modelling and visualization of geological outcrops. *International Archives of the Photogrammetry, Remote Sensing and Spatial Information Sciences*, **37**, 493–498.

Cartwright, J. & Hansen, D.M. 2006. Magma transport through the crust via interconnected sill complexes. *Geology*, **31**, 929–932.

Cartwright, J. & Huuse, M. 2005. 3D seismic technology: the geological 'Hubble'. *Basin Research*, **17**, 1–20, http://doi.org/10.1111/j.1365-2117.2005.00252.x.

Dam, G. & Surlyk, F. 1998. *Stratigraphy of the Neill Klinter Group; a Lower–lower Middle Jurassic tidal embayment succession, Jameson Land, East Greenland*. Geology of Greenland Survey Bulletin, **175**.

Delaney, P.T. & Gartner, A.E. 1997. Physical processes of shallow mafic dike emplacement near the San Rafael Swell, Utah. *Geological Society of America Bulletin*, **109**, 1177–1192.

Doré, A. G. 1992. Synoptic palaeogeography of the Northeast Atlantic Seaway: Late Permian to Cretaceous. *In*: Parnell, J. (ed.) *Basins on the Atlantic seaboard: petroleum geology, sedimentology and basin evolution*. Geological Society, London, Special Publication, **62**, 421–446.

Eide, C.H., Howell, J.A., Buckley, S.J., Martinius, A.W., Oftedal, B.T. & Henstra, G.A. 2016. Facies model for a coarse-grained, tide-influenced delta: Gule Horn Formation (Early Jurassic), Jameson Land, Greenland. *Sedimentology*, first published online May 25, 2016, http://doi.org/10.1111/sed.12270.

Galland, O., Planke, S., Neumann, E.-R. & Malthe-Sørenssen, A. 2009. Experimental modelling of shallow magma emplacement: Application to saucer-shaped intrusions. *Earth and Planetary Science Letters*, **277**, 373–383.

Gjelberg, J., Dreyer, T., Høie, A., Tjelland, T. & Lilleng, T. 1987. Late Triassic to Mid-Jurassic sandbody development on the Barents and mid-Norwegian shelf. *In*: Brooks, J. & Glennie, K.W. (eds) *Petroleum Geology of North West Europe. Proceedings of the 3rd Conference*. Geological Society, London, 1105–1129.

Hald, N. & Tegner, C. 2000. Composition and age of Tertiary sills and dykes, Jameson Land Basin, East Greenland: relation to regional flood volcanism. *Lithos*, **54**, 207–233.

Hamann, N.E., Whittaker, R.C. & Stemmerik, L. 2005. Geological development of the Northeast Greenland Shelf. *In*: Doré, A.G. & Vining, B.A. (eds) *Petroleum Geology: North-West Europe and Global Perspectives—Proceedings of the 6th Petroleum Geology Conference*. Geological Society, London, 887–902, http://doi.org/10.1144/0060887

Hansen, D.M. & Cartwright, J. 2006. Saucer-shaped sill with lobate morphology revealed by 3D seismic data: implications for resolving a shallow-level sill mechanism. *Journal of the Geological Society, London*, **163**, 509–523, http://doi.org/10.1144/0016-764905-073

Hansen, J., Jerram, D.A., McCaffrey, K. & Passey, S.R. 2009. The onset of the North Atlantic Igneous Province in a rifting perspective. *Geological Magazine*, **146**, 309–325.

Hansen, J., Jerram, D.A., McCaffrey, K. & Passey, S.R. 2011. Early Cenozoic saucer-shaped sills of the Faroe Islands: an example of intrusive styles in basaltic lava piles. *Journal of the Geological Society, London*, **168**, 159–178, http://doi.org/10.1144/0016-76492010-012

Hansen, K., Bergman, S.C. & Henk, B. 2001. The Jameson Land basin (east Greenland): a fission track study of the tectonic and thermal evolution in the Cenozoic North Atlantic spreading regime. *Tectonophysics*, **331**, 307–339.

Hersum, T.G., Marsh, B.D. & Simon, A.C. 2007. Contact partial melting of granitic country rock, melt segregation, and re-injection as dikes into Ferrar Dolerite Sills, McMurdo Dry Valleys, Antarctica. *Journal of Petrology*, **48**, 2125–2148.

Holford, S.P., Schofield, N., Jackson, C.A.-L., Magee, C., Green, P.F. & Duddy, I.R. 2013. Impacts of igneous intrusions on source and reservoir potential in prospective sedimentary basins along the Western Australian continental margins. *In*: Keep, M. & Moss, S.J. (eds) *West Australian Basins Symposium. Proceedings of the Petroleum Exploration Society of Australia Symposium*, Perth, WA, 1–12.

Hutton, D.H.W. 2009. Insights into magmatism in volcanic margins: bridge structures and a new mechanism of basic sill emplacement—Theron Mountains, Antarctica. *Petroleum Geoscience*, **15**, 269–278.

Ichaso, A.A. & Dalrymple, R.W. 2014. Eustatic, tectonic and climatic controls on an early syn-rift mixed-energy delta, Tilje Formation (Early Jurassic, Smørbukk field, offshore mid-Norway). *In*: Brooks, A.W., Ravnås, R., Howell, J.A., Steel, R.J. & Wonham, P. (eds) *From Depositional Systems to Sedimentary Successions on the Norwegian Continental Margin*. International Association of Sedimentologists, Special Publication, **46**, 339–388.

Jackson, C.A., Schofield, N. & Golenkov, B. 2013. Geometry and controls on the development of igneous sill-related forced folds: A 2-D seismic reflection case study from offshore southern Australia. *Geological Society of America Bulletin*, **125**, 1874–1890, http://doi.org/10.1130/B30833.1

Jerram, D.A. & Bryan, S.E. 2015. Plumbing systems of shallow level intrusive complexes. *In*: Breitkreuz, C.H. & Rocchi, S. (eds) *Physical Geology of Shallow Magmatic Systems.* Advances in Volcanology. Springer, Berlin, 1–22, http://doi.org/10.1007/11157_2015_8.

Jerram, D.A. & Stollhofen, H. 2002. Lava/sediment interaction in desert settings; are all peperite-like textures the result of magma–water interaction? *Journal of Volcanology and Geothermal Research*, **114**, 231–249.

Jerram, D.A. & Widdowson, M. 2005. The anatomy of continental flood basalt provinces: geological constraints on the processes and products of flood volcanism. *Lithos*, **79**, 385–405.

Jerram, D.A., Single, R.T., Hobbs, R.W. & Nelson, C.E. 2009. Understanding the offshore flood basalt sequence using onshore volcanic facies analogues: an example from the Faroe–Shetland basin. *Geological Magazine*, **146**, 353–367.

Jerram, D.A., Davis, G.R., Mock, A., Charrier, A. & Marsh, B.D. 2010. Quantifying 3D crystal populations, packing and layering in shallow intrusions: a case study from the Basement Sill, Dry Valleys, Antarctica. *Geosphere*, **6**, 537–548.

Jerram, D.A., Svensen, H.H., Planke, S., Polozov, A.G. & Torsvik, T.H. 2016. The onset of flood volcanism in the north-western part of the Siberian Traps: Explosive volcanism versus effusive lava flows. *Palaeogeography, Palaeoclimatology, Palaeoecology*, **441**, 38–50.

Kavanagh, J.L., Menand, T. & Sparks, S.J. 2006. An experimental investigation of sill formation and propagation in layered elastic media. *Earth and Planetary Science Letters*, **254**, 799–813.

Krabbe, H., Christiansen, F.G., Dam, G., Piasecki, S. & Stemmerik, L. 1994. Organic geochemistry of the Lower Jurassic Sortehat Formation, Jameson Land, East Greenland. *Rapport Grønlands Geologiske Undersøgelse*, **164**, 5–19.

Larsen, H.C. & Marcussen, C. 1992. Sill-intrusion, flood basalt emplacement and deep crustal structure of the Scoresby Sund Region, East Greenland. *In*: Storey, B.C., Alabaster, T. & Pankhurst, R.J. (eds) *Magmatism and the Causes of Continental Break-up*. Geological Society, London, Special Publication, **68**, 365–368, http://doi.org/10.1144/GSL.SP.1992.068.01.23

Larsen, M.L., Watt, W.S. & Watt, M. 1989. *Geology and petrology of the Lower Tertiary plateau basalts of the Scoresby Sund region, East Greenland*. Grønlands Geologiske Undersøgelse Bulletin, **157**.

Lecomte, I., Lavadera, P.L. *et al.* 2016. 2(3)D convolution modelling of complex geological targets beyond 1D convolution. *First Break*, **34**, 99–107.

Magee, C., Maharaj, S.M., Wrona, T. & Jackson, C.A.L. 2015. Controls on the expression of igneous intrusions in seismic reflection data. *Geosphere*, **11**, 1024–1041.

Magee, C., Muirhead, J.D. *et al.* 2016. Lateral magma flow in mafic sill complexes. *Geosphere*, **12**, 809–841.

Martinius, A.W., Kaas, I., Næss, A., Helgesen, G, Kjærefjord, J.M. & Leith, D.A. 2001. Sedimentology of the heterolithic and tide-dominated Tilje Formation (Early Jurassic, Halten Terracce, offshore mid-Norway). *In*: Martinsen, O.J. & Dreyer, T. (eds) *Sedimentary Environments Offshore Norway—Palaeozoic to Recent*. Norwegian Petroleum Society Special Publication, **10**, 103–144.

Mathiesen, A., Bidstrup, T. & Christiansen, F.G. 2000. Denudation and uplift history of the Jameson Land basin, East Greenland—constrained from maturity and apatite fission track data. *Global and Planetary Change*, **24**, 275–301.

Mjelde, R., Breivik, A.J., Raum, T., Mittelstaedt, E., Ito, G. & Faleide, J.I. 2008. Magmatic and tectonic evolution of the North Atlantic. *Journal of the Geological Society, London*, **165**, 31–42, http://doi.org/10.1144/0016-76492007-018

Mudge, M.R. 1968. Depth control of some concordant intrusions. *Geological Society of America Bulletin*, **79**, 315–322.

Nelson, C.E., Jerram, D.A., Clayburn, J.A.P., Halton, A.M. & Roberge, J. 2015. Eocene volcanism in offshore southern Baffin Bay. *Marine and Petroleum Geology*, **67**, 678–691.

Noe-Nygaard, A. 1976. Tertiary igneous rocks between Shannon and Scoresby Sund East Greenland. *In*: Escher, A. & Watt, W.S. (eds) *Geology of Greenland*. Grønlands Geologiske Undersøgelse, Copenhagen, 386–402.

Oelkers, E.H., Bjørkum, P.A. & Murphy, W.M. 1996. A petrographic and computational investigation of quartz cementation and porosity reduction in North Sea sandstones. *American Journal of Science*, **296**, 420–452.

Planke, S., Rasmussen, T., Rey, S.S. & Myklebus, R. 2005. Seismic characteristics and distribution of volcanic intrusions and hydrothermal vent complexes in the Vøring and Møre basins. *In*: Doré, A.G. & Vining, B.A. (eds) *Petroleum Geology: North-West Europe and Global Perspectives—Proceedings of the 6th Petroleum Geology Conference*. Geological Society, London, 833–844, http://doi.org/10.1144/0060833

Pollard, D.D. 1973. Derivation and evaluation of a mechanical model for sheet intrusions. *Tectonophysics*, **19**, 233–269.

Polozov, A.G., Svensen, H.H., Planke, S., Grishina, S.N., Fristad, K.E. & Jerram, D.A. 2016. The basalt pipes of the Tunguska Basin (Siberia, Russia): High temperature processes and volatile degassing into the end-Permian atmosphere. *Palaeogeography, Palaeoclimatology, Palaeoecology*, **441**, 51–64.

Polteau, S., Mazzini, A., Galland, O., Planke, S. & Malthe-Sørenssen, A. 2008. Saucer-shaped intrusions: Occurrences, emplacement and implications. *Earth and Planetary Science Letters*, **266**, 195–204.

Rickwood, P.C. 1990. The anatomy of a dyke and the determination of propagation and magma flow directions. *In*: Parker, A.J., Rickwood, P.C. & Tucker, D.H. (eds) *Mafic Dykes and Emplacement Mechanisms*. Balkema, Rotterdam, 81–100.

Rittersbacher, A., Buckley, S.J., Howell, J.A., Hampson, G.J. & Vallet, J. 2014. Helicopter-based laser scanning: a method for quantitative analysis of large-scale sedimentary architecture. *In*: Martinius, A.W., Howell, J.A. & Good, T. (eds) *Sediment-Body Geometry and Heterogeneity: Analogue Studies for Modelling the Subsurface*. Geological Society, London, Special Publications, **387**, 185–202, http://doi.org/10.1144/SP387.3

Saunders, A.D., Fitton, J.G., Kerr, A.C., Norry, M.J. & Kent, R.W. 1997. The North Atlantic Igneous Province. *In*: Mahoney, J.J. & Coffin, M. F. (eds) *Large Igneous Provinces: Continental, Oceanic, and Planetary Flood Volcanism*. Geophysical Monograph, American Geophysical Union, **100**, 45–93.

Schofield, N., Stevenson, C. & Reston, T. 2010. Magma fingers and host rock fluidization in the emplacement of sills. *Geology*, **38**, 63–66.

Schofield, N.J., Brown, D.J., Magee, C. & Stevenson, C.T. 2012*a*. Sill morphology and comparison of brittle and non-brittle emplacement mechanisms. *Journal of the Geological Society, London*, **169**, 127–141, http://doi.org/10.1144/0016-76492011-078

Schofield, N., Heaton, L., Holford, S.P., Archer, S.G., Jackson, C.A.-L. & Jolley, D.W. 2012*b*. Seismic imaging of 'broken bridges': linking seismic to outcrop-scale investigations of intrusive magma lobes. *Journal of the Geological Society, London*, **169**, 421–426, http://doi.org/10.1144/0016-76492011-150

Schofield, N., Alsop, I., Warren, J., Underhill, J.R., Lehné, R., Beer, W. & Lukas, V. 2014. Mobilizing salt: Magma–salt interactions. *Geology*, **42**, 599–602.

Schofield, N., Holford, S. *et al.* 2015. Regional magma plumbing and emplacement mechanisms of the Faroe–Shetland Sill Complex: implications for magma transport and petroleum systems within sedimentary basins. *Basin Research*, first published online November 19, 2015, http://doi.org/10.1111/bre.12164

Schofield, N., Jerram, D.A. *et al.* 2016. Sills in sedimentary basins and petroleum systems. *In*: Breitkreuz, C.H. & Rocchi, S. (eds) *Physical Geology of Shallow Magmatic Systems*. Advances in Volcanology. Springer, Berlin, first published online April 5, 2016, http://doi.org/10.1007/11157_2015_17.

Skilling, I.P., White, J.D.L. & McPhie, J. 2002. Peperite: a review of magma–sediment mingling. *Journal of Volcanology and Geothermal Research*, **114**, 1–17.

Stemmerik, L., Dam, G., Noe-Nygaard, N., Piasecki, S. & Surlyk, F. 1998. Sequence stratigraphy of source and reservoir rocks in the Upper Permian and Jurassic of Jameson land, East Greenland. *Geology of Greenland Survey Bulletin*, **180**, 43–54.

Surlyk, F. 2003. The Jurassic of East Greenland: a sedimentary record of thermal subsidence, onset and culmination of rifting. *In*: Ineson, J.R. & Surlyk, F. (eds)

The Jurassic of Denmark and Greenland. Geological Survey of Denmark and Greenland Bulletin, **1**, 659–722.

Svensen, H., Polteau, S., Cawthorn, G. & Planke, S. 2015. Sub-volcanic intrusions in the Karoo Basin, South Africa. *In*: Breitkreuz, C.H. & Rocchi, S. (eds) *Physical Geology of Shallow Magmatic Systems*. Advances in Volcanology, Springer, Berlin, first published online January 13, 2015, http://doi.org/10.1007/11157_2014_7

Talwani, M. & Eldholm, O. 1977. Evolution of the Norwegian–Greenland sea. *Geological Society of America Bulletin*, **88**, 969–999.

Torsvik, T.H., Mosar, J. & Eide, E.A. 2001. Cretaceous–Tertiary geodynamics: a North Atlantic exercise. *Geophysical Journal International*, **146**, 850–866.

Vallet, J. & Skaloud, J. 2004. Development and experiences with a fully-digital handheld mapping system operated from a helicopter. *International Archives of the Photogrammetry, Remote Sensing and Spatial Information Sciences*, **35** (Part B), 1–6.

Ziegler, P. 1988. Evolution of the Arctic – North Atlantic and the western Tethys. *American Association of Petroleum Geologists Memoir*, **43**.